Enhanced Biological Activity of Metal Nanoparticles-

(+) Catechin Bioconjugate with Protein

By

V.SNEKA

(20PPH021)

A Thesis submitted to

Avinashilingam Institute for Home Science and Higher Education for Women Coimbatore-641 043

In partial fulfilment of the requirements for the degree of

MASTER OF SCIENCE IN PHYSICS

MAY 2022

Enhanced Biological Activity of Metal Nanoparticles-

(+) Catechin Bioconjugate with Protein

By

V.SNEKA

(20PPH021)

A Thesis submitted to

Avinashilingam Institute for Home Science and Higher Education for Women Coimbatore-641 043

In partial fulfilment of the requirements for the degree of

MASTER OF SCIENCE IN PHYSICS

MAY 2022

CERTIFIED AS A BONAFIDE RESEARCH WORK

27/05/22

Signature of the Head of the Department

27/5/22

Signature of the Supervisor

ACKNOWLEDGEMENT

ACKNOWLEDGEMENT

I owe my sincere thanks to **Lord Almighty** and **My Parents** without whom I would have been nothing and showering their generous blessings upon me in all endeavors

I wish to express my deep sense of reverential gratitude to **Prof.S.P.THYAGARAJAN**, Chancellor, Avinashilingam Institute for Home Science and Higher Education for Women, Coimbatore, for providing the facilities to conduct this study.

I extend my thanks to **HON.Dr.V.BHARATHI HARISHANKAR**, Vice Chancellor, Avinashilingam Institute for Home Science and Higher Education for Women, Coimbatore, for providing flamboyant help towards the completion of the study.

I record my deep sense of gratitude and indebtedness to **Dr.S.KOWSALYA, Registrar**, Avinashilingam Institute for Home Science and Higher Education for Women, Coimbatore, for providing adequate help for the study.

I also wish to express my gratitude to **Dr.(Mrs).G.PADMAVATHI,** Dean, school of physical sciences and computational sciences, Avinashilingam Institute for Home Science and Higher Education for Women, Coimbatore, for timely help rendered throughout the course.

I whole heartily thank **Dr.J.SHANTHI**, Professor and Head of the Department of Physics, Avinashilingam Institute for Home Science and Higher Education for Women, Coimbatore, for her encouragement and generous help which was of great value.

I are very much indebted to my Guide, **Mrs.S.ANITHA**, Assistant Professor, Department of Physics, Avinashilingam Institute for Home Science and Higher Education for Women, Coimbatore, for her excellent, outstanding guidance, constructive criticism, motivation, valuable advice, untiring support, timely suggestions, holding me strong in all the places when we faltered.

I thank **Dr.V.SASIREKHA** and **all the staff members of the Department of Physics**, Avinashilingam Institute for Home Science and Higher Education for Women, Coimbatore, for being untiring support and guidance.

I also express my gratitude to **TAMILNADU STATE COUNCIL FOR SCIENCE AND TECHNOLOGY** for sanctioning student project (PS-334) 2021-2022

I thank all my friends for their support, understanding and co-operation for the successful completion of the study.

SNEKA.V

LIST OF CONTENTS

CONTENTS

LIST OF FIGURES

LIST OF TABLES

CHAPTER – I

1.1 INTRODUCTION

Albumin is the most abundant protein in the vertebrate's organisms (up to 40 mg/ml) and the most prominent plasma protein (about 60% of the total protein content of plasma). It is one of the first discovered and most intensely studied proteins [1]. Plasma proteins act as carriers for transportation of drugs and other compounds. Amongst the various plasma proteins, serum albumin is the most abundant protein and it plays a vital role in transportation of drug ligands [2]. Serum albumin is a protein found in blood plasma and carries proteins for Steroids, Fatty-acids and thyroid hormones. It plays an important role in stabilizing cellular volume with help of Colloid osmotic pressure. Serum albumin had a good binding capacity, fatty acids, hormones, bilirubin and drugs etc. The interaction of drug with protein is essential to design new drugs and improve the therapeutic efficacy. Bovine serum albumin (BSA) has been used as a model protein to study drug interaction, 75 % structural homology with that of human serum albumin (HSA). Serum albumin levels are widely regarded as a marker of nutritional status but may also be reduced due to proteinuria or inflammation.[3] Serum albumin is the most important biochemical index of malnutrition. Significant decreases in levels of serum albumin reflect chronic protein depletion; however, they are poor measures of early protein malnutrition because of the long half-life of serum albumin (20 days) and large total body pool of albumin.[4]. The serum albumin concentration is used to evaluate chronic liver disease and hepatocellular function (protein synthesis). Serum albumin is a water-soluble, anionic globular protein of molecular weight ~65,000 [5]. Serum albumin is the best-studied serum protein and has prognostic value for subsequent mortality and morbidity in community-dwelling older person. Because serum albumin does not fall quickly (half-life 18-21 days) in protein deprivation, it may be quite a useful indicator for chronic moderate to severe under nutrition. In contrast, proteins with shorter half-lives such as prealbumin (half-life 2-3 days) and transferrin (half-life 8-9 days) may respond to nutritional interventions more quickly and may be better for monitoring treatment.[6]

Serum albumin is produced by the liver, occurs dissolved in blood plasma and is the most abundant blood protein in mammals. Albumin is essential for maintaining the oncotic pressure needed for proper distribution of body fluids between blood vessels and body tissues; without albumin, the high pressure in the blood vessels would force more fluids out into the

tissues. It also acts as a plasma carrier by non-specifically binding several hydrophobic steroid hormones and as a transport protein for hemin and fatty acids. Too much or too little circulating serum albumin may be harmful. Serum albumin is widely distributed in mammals.

- The human version is human serum albumin.
- BSA, is commonly used in immunodiagnostic procedures, clinical chemistry reagents, cell culture media, protein chemistry research and molecular biology laboratories.

1.2 Bovine Serum Albumin

BSA is a serum albumin protein derived from cows. BSA is commonly used in cell culture protocols, particularly where protein supplementation is necessary and the other serum components are unwanted. Cell culture, it acts as a small molecule carrier. The BSA molecule consists of 583 amino acids, bound in a single chain cross-linked with 17 cysteine residues (eight disulfide bonds and one free thiol group), and has a molecular mass of 66400 Da . The amino acid chain is made up of three homologous but structurally distinct domains (I, II and III), divided into nine loops by the disulfide bonds and arranged in a heart-shaped molecule shown in Fig 1.1. Each domain consists of two sub-domains, A and B. The secondary structure of the protein is mainly α-helical (74%), with the remaining polypeptide chain occurring in turns and in extended or flexible regions between subdomains. BSA shows discrete binding sites with different specificities, the most important ones being referred to as site-I and site-II, located in hydrophobic cavities of subdomains IIA and IIIA, respectively which is shown in fig 1.1. Site markers are small molecules that have specific binding locations in the albumin structure and are often used in studying the interaction of different ligands with the protein. Site-I markers include warfarin, phenylbutazone, dansylamide and iodipamide, while ibuprofen, flufenamic acid and diazepam are site-II markers. [1]

1.2.1 Properties of Bovine Serum Albumin

Serum albumin are the major native carrier found in the blood and involved in the transporting and delivering of exogenous and endogenous materials (fatty acids, nutrients, steroids, and a variety of therapeutic drug). It must be noted that the effectiveness of drug solubility, bio distribution and their interaction is highly affected by their binding nature and interaction with protein. Strong binding can decrease the concentration of free drugs in plasma where as weak binding may lead to poor distribution and had short life time.

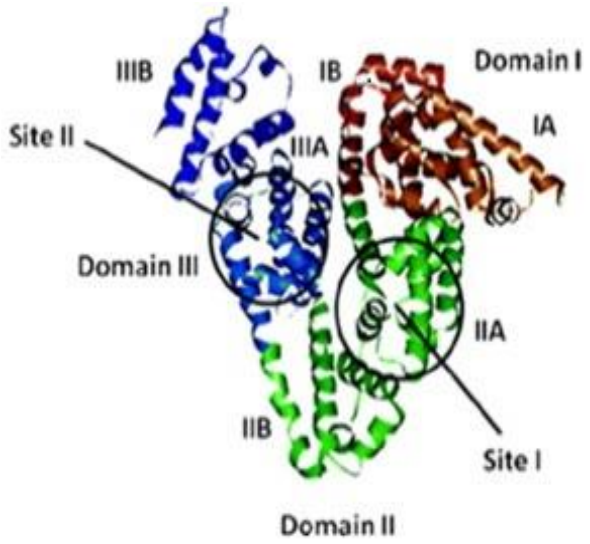

Fig 1.1 Structure of Bovine Serum Albumin

1.2.2 USES

- BSA in bovine milk has also been implicated in the allergic reactions in humans to bovine milk and has even been investigated as a possible cause for the stimulation of autoimmune disease leading to insulin-dependent diabetes mellitus in humans.
- BSA (often from a fetal bovine source) is also used as a nutrient in cell and microbial culture. In molecular biology, BSA is used to stabilize some restriction enzymes during digestion of DNA and to prevent adhesion of the enzyme to reaction tubes, pipet tips, and other vessels.
- BSA has been used as a model protein to study drug interaction, 75 % structural homology with that of HSA.

1.3 Amino Acid

Amino acids are the monomers that make up proteins. Each amino acid has the same fundamental structure , which consists of a central carbon atom, also known as the alpha (α) carbon, bonded to an amino group (NH_2), a carboxyl group (COOH), and to a hydrogen atom shown in fig 1.2. In the aqueous environment of the cell, the both the amino group and the carboxyl group are ionized under physiological conditions, and so have the structures -NH_3^+ and -COO^-, respectively. Every amino acid also has another atom or group of atoms bonded to the central atom known as the R group. This R group, or side chain, gives each amino acid proteins specific characteristics, including size, polarity, and pH. In the form of proteins, amino

acids comprise the second-largest component (water is the largest) of human muscles, cells and other tissues. Outside proteins, amino acids perform critical roles in processes such as neurotransmitter transport and biosynthesis.

The key elements of an amino acid are carbon (C), hydrogen (H), oxygen (O), and nitrogen (N), although other elements are found in the side chains of certain amino acids. About 500 naturally occurring amino acids are known as of 1983 (though only 20 appear in the genetic code) and can be classified in many ways. They can be classified according to the core structural functional groups' locations as alpha- (α-), beta- (β-), gamma- (γ-) or delta- (δ) amino acids; other categories relate to polarity, pH level, and side chain group type (aliphatic, acyclic, aromatic, containing hydroxyl or sulfur, etc.). In the form of proteins, amino acid residues form the second-largest component (water is the largest) of human muscles and other tissues. Beyond their role as residues in proteins, amino acids participate in a number of processes such as neurotransmitter transport and biosynthesis.

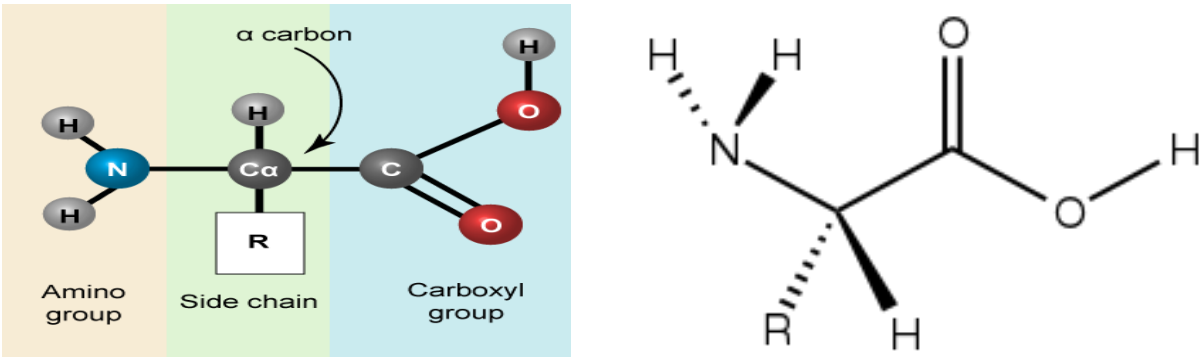

Fig 1.2 Structure of amino acid

1.4 Natural Products

The Natural Product is an organic compound that is synthesized by a living organism. Natural products and their derivatives are commonly used as food additives in the form of spices and herbs, antibacterial agents, and antioxidants to protect food freshness and longevity. Natural Products are secondary metabolites that are regarded as the readouts of developmental or physiological status of an organism [7]. The total number of plant metabolites is estimated to exceed 200000 reflecting the extraordinary diversity of functions that natural products may serve. Plant metabolites play essential roles in growth, cellular condition and whole plant resource allocation as well as in their interactions with the environment. Among the

phytochemicals mentioned as potentially providing health benefits are polyphenols, flavonoids, isoflavonoids, anthocyanidins, phytoestrogens, terpenoids, carotenoids, limonoids, phytosterols, glucosinolates, and fibres [8]. In addition, they provide indispensable resources for human nutrition, energy and medicine.

Plant metabolites can be conceptually divided into two categories.

- Primary metabolites
- Secondary metabolites

1.4.1 Primary Metabolites

Primary metabolites such as carbohydrates, amino acids, fatty acids, and organic acids are involved in growth, respiration, photosynthesis, protein synthesis and hormone. Primary metabolites are found across all species within broad phylogenetic groups and produced using the same biochemical pathways.

1.4.2 Secondary Metabolites

Secondary metabolites such as flavonoids, carotenoids, sterols, phenolic acids, alkaloids, and glucosinolates determine the color of vegetables, protect plants against herbivores and microorganisms, attract pollinators, seed dispersing animals and act as signal molecules under stress conditions [9].

1.5 Polyphenols

Polyphenols are a category of compounds naturally found in plant foods, such as fruits, vegetables, herbs, spices, tea, dark chocolate, and wine.Polyphenols is briefly classified into several categories. Fruits like grapes, apple, pear, cherries and berries contains up to 200–300 mg polyphenols per 100 grams fresh weight. The products manufactured from these fruits, also contain polyphenols in significant amounts. Polyphenols are secondary metabolites of plants and are generally involved in defense against ultraviolet radiation or aggression by pathogens. In food, polyphenols may contribute to the bitterness, astringency, color, flavor, odor and oxidative stability. [10] There are more than 8,000 types of polyphenols, which includes flavanoids, polyphenolic amides, phenolic acids. Polyphenols help protect your body by Improving Heart Health, Lowering Diabetes Risk, Anticancer Properties, raising Immunity. Most plant-based foods contain polyphenols, like vegetables, fruits, and whole grains. It’s easy to get enough in diet to boost your health, but some sources are more nutritious than others.[11].

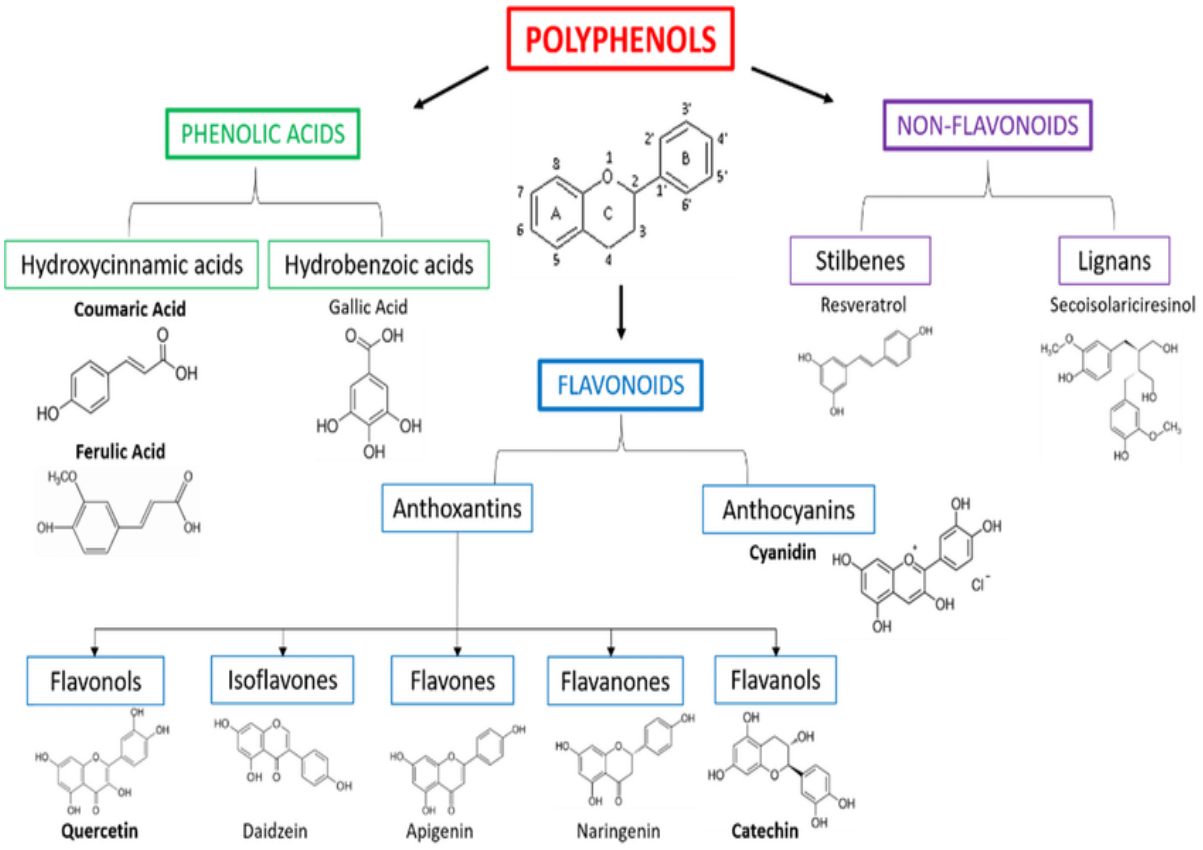

Fig 1.3 Classification of Polyphenols

1.5.1 Flavonoids

Flavonoids, a group of natural substances with variable phenolic structures, are found in fruits, vegetables, grains, bark, roots, stems, flowers, tea and wine. Chemically flavonoids are based upon a fifteen-carbon skeleton consisting of two benzene rings (A and C) linked via a heterocyclic pyrane ring (B)[18]. They are a colourless molecule that accumulates mainly in the outer and aerial tissues, skin and leaves of fruit and vegetables. The C15H10O3 is the molecular formula of flavonols [19]. The structure of flavonoids is a skeleton of diphenyl propane, with two benzene rings linked by a three-carbon chain, which forms a closed pyran ring (heterocyclic ring containing oxygen, the C ring) with benzenic A ring, referred to as C6-C3-C6 [12].

1.5.2 Flavones

Flavones are a group of flavonoids that contain a 2-phenyl-1-benzopyran-4-one skeleton. The flavones are commonly present in herbs such as parsley and celery, maize, wheat, rye, barley, oats, sorghum, and millets. [13].

1.5.3 Flavonols

Flavonols are the most ubiquitous flavonoids in foods, the main representatives being quercetin, kaempferol, and myricetin. They are present mainly in onions18 at concentrations up to 1.2 g kg−1 fresh weight, but also in kale, leeks and broccoli.[14]

1.5.4 Flavanones

Flavanones have the basic 2,3-dihydroflavone structure and lack a double bond between C2 and C3; this makes them chiral at the C2 position. The chirality implies the B-ring is twisted relative to the A-C rings and is not planar like the conjugated flavones. [15]

1.5.5 Isoflavones

Isoflavones are a subclass of flavonoids, they are the major phytoestrogens naturally found in plants. Isoflavones are mainly present in soybeans (5–30 mg/100 g) which are which are the 3-hydroxy position 3 of the C ring.[16]

1.6 (+) Catechins

Flavanols or flavan-3-ols are often commonly called (+) catechins (CT). CT is a flavan-3-ol, a type of natural phenol and antioxidant. It is a plant secondary metabolite. It belongs to the group of flavan-3-ols, part of the chemical family of flavonoids. CT is a polyphenolic phytochemicals found in green tea and cocoa fruits. CT play important role in inflammatory autoimmune myocarditis. The main structural difference from other flavonoids is the absence of a double bond between C2 and C3 in flavanols, and no C4 carbonyl in ring C. CT possesses two benzene rings (called the A- and B-rings) and a dihydropyran heterocycle (the C-ring) with a hydroxyl group on carbon 3. The A ring is similar to a resorcinol moiety while the B ring is similar to a catechol moiety.[17] The structures of CT is constituted by resorcinol (A ring) and catechol (B ring) moiety, which are interconnected by a benzopyran ring (C ring). Molecular formula of CT is $C_{15}H_{14}O_{16}$ and its molecular weight is 290.27. Its molecular structure is shown in the Fig 1.4 a.

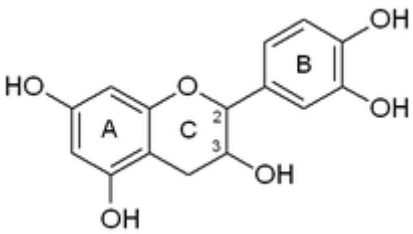

Fig 1.4 Structure of (+) Catechin

1.6.1 Applications of (+) Catechin

In recent years, CT have been used as natural antioxidant in oils and fats against lipid oxidation, supplement for animal feeds both to improve animal health and to protect animal products, an antimicrobial agent in foodstuffs and a health functional ingredient in various foods and dietary supplements [18].The effects of CT on the human body and boost their protective power against UV radiation. There are many examples of the positive anti-microbial, anti-viral, anti-inflammatory, anti-allergenic, and anti-cancer effects of CT. CT increase the penetration and absorption of healthy functional foods and bio cosmetics into the body and the skin, thus improving their utility. High value-added anti-oxidant substances have been extracted from food and plant sludge, and experiments have shown that CT are safe when applied to the human body. The stability of CT is very important for their absorption into the human body and the effectiveness of their anti-oxidant properties [19].

1.7 Nanotechnology

At present, nanobiotechnology, which is a combination of nanotechnology, biotechnology, chemical processing, material science, and system engineering, is one of the fastest developing research areas. The use of nanoparticles (NPs), especially gold and silver, in commercial and medicinal applications has rapidly increased within the last decade due to their fascinating properties and intriguing applications, such as biosensing, medical imaging, cancer nanomedicine, and paints. Conventional techniques, routes, and methodologies used for the synthesis of these nanoparticles have come under scrutiny due to the use or production of hazardous chemicals, products, by-products, reagents and solvents. Therefore, greener and more eco-friendly techniques are being investigated for nanoparticle synthesis worldwide, using plant and fruit extracts, bacteria, fungi, yeast, and algae. Green chemistry provides an environmentally compatible scheme for the fabrication of functional metal NPs. Recently,

polyphenols obtained from plants, fruits, and vegetables have garnered interest for the synthesis of metal NPs. From a biological and medicinal point of view, the principal interest in nanoparticle is rooted in the concept that due to their relatively small size, they can communicate with cellular machinery and possibly enter previously inaccessible target locations, such as the brain. Therefore, when looking at the potential in vivo applications of nanoparticles, the recognition and control of these nanoparticle-protein interactions in the bloodstream are of prime importance. [20]

1.7.1 Nanoparticles

Nanoparticles (NPs) are wide class of materials that include particulate substances, which have one dimension less than 100 nm at least. Depending on the overall shape these materials can be 0D, 1D, 2D or 3D [21]. NPs exist in the natural world and are also created as a result of human activities. Because of their sub microscopic size, they have unique material characteristics, and manufactured nanoparticles may find practical applications in a variety of areas, including medicine, engineering, catalysis, and environmental remediation. NPs can be classified into any of various types, according to their size, shape, and material properties. Some classifications distinguish between organic and inorganic nanoparticles. . Nanomaterial's possess several unique features including (1) submicron sizes, (2) surface charge, (3) colloidal stability, (4) high encapsulation efficiency, (5) improved solubility, (6) target-specific delivery, (7) alleviated off-target effects, (8) halting systemic toxicity, (9) improved pharmacokinetic profile, and (10) optimized therapeutic efficacy. Amongst different types of nanomaterial's, silver nanoparticles (NPs) (SNPs) are widely employed nanomaterial's, which have gained enormous viability.

1.7.2 Metal Nanoparticles

Metal NPs (MNPs) play a major role in nanotechnology and nanoscience. MNPs have been found to play a major role in the medical, biomedical, and pharmaceutical applications of nanotechnology. They proved to be effective in the delivery of drugs, proteins, peptides, and genes. MNPs have a metal core composed of inorganic metal or metal oxide that is usually covered with a shell made up of organic or inorganic material or metal oxide. MNPs have diverse application in our daily life. MNPs are widely used to synthesise metal based biopolymer composites because of properties of metal nanoparticles including optical polarizability, antibacterial activity, electrical conductivity, chemical properties and

biocompatibility. MNPs and their technological applications in various fields of science have become a topic of importance for the global research community. The selective and reproducible synthesis of MNPs is imperative for wide applications. Various chemical and biological methods are used for the synthesis of metal nanoparticles.

1.7.3 Need for green synthesis and silver nanoparticles

Silver is a basic element which is non-toxic belonging thermal and electrical potential. Silver demand will likely to rise as silver find new uses, particularly in textiles, plastics and medical industries, surgical, dental resigns, coated water filters, sanitizers, detergents, soap and wound dressings. Applicability in healthcare for treatment of mental illness, convulsions, de addiction of narcotic products along with sexually transmitted diseases like syphilis and gonorrhea leads to changing the pattern of silver emission as these technologies and products diffuse through the global economy. Green synthesis is an emerging approach which overcomes demerits of physiochemical approaches by utilization of natural herbs which are nontoxic. Green synthesized nanosilver offer many advantages like utilization of phytochemicals, antioxidants acts as naturally occurring reducing agents, coast efficient, large scale manufacturing highly beneficial and usage of toxic chemicals, high pressure, energy are avoided. Nano silver can be engineered by different techniques such as irradiation, reduction, electrochemical and chryochemical synthesis. Nanosilver can be molded in to desired shapes and bear unique properties like permeability by pH and dissolved ions as compare to routine metals. As Silver nanoparticles generate larger surface area per unit mass which improves contact time nanosilver customer market an demand drastically raised in wide verity of industries along with healthcare, food packing, textiles, cosmetics etc.[22]

1.8.4 Silver Nanoparticles

Nitrate group of silver potentially responsible for its broad spectrum antibacterial potential and as it convert in to Silver nanoparticles (AgNPs) surface area is drastically increased which improve microbial exposure time and area. AgNPs are increasingly used in various fields, including medical, food, health care, consumer, and industrial purposes, due to their unique physical and chemical properties. Generally AgNPs are nanoparticles of silver having size range between 1 and 100 nm in size having unique properties such as electrical, optical and magnetic having wide range of applicability. Green chemistry is and encouraging approach mainly utilize nanosilver along with natural biomolecules such as polysaccharides, tollens which overcomes drawbacks of conventional methods and produce AgNPs which are

ecofriedly, nontoxic and coast effective. Ionic silver is active form of silver which binds to cell wall of bacteria leading to major structural changes in cell morphology. Silver is also called as oligodynamic due to its bactericidal potential at minimum concentration. [23]. Various biomedical implications such as wound healing, antibacterial, antifungal, anticancer, antiproliferative, antiinflammatory, antioxidant, antiviral, and antidiabetic properties [22]

1.8.5 Properties of AgNPs

Physical and chemical properties of AgNPs—including surface chemistry, size, size distribution, shape, particle morphology, particle composition, coating/capping, agglomeration, dissolution rate, particle reactivity in solution, efficiency of ion release, cell type, and finally type of reducing agents used for synthesis—are crucial factors for determination of cytotoxicity. AgNP toxicity mainly depends on the availability of chemical and or biological coatings on the nanoparticle surface. AgNP surface charges could determine the toxicity effect in cells. For instance, the positive surface charge of these NPs renders them more suitable, allowing them to stay for a long time in blood stream compared to negatively-charged NPs, which is a major route for the administration of anticancer agents.

1.8.6 Biological Applications of AgNPs

Due to their unique properties, AgNPs have been used extensively in house-hold utensils, the health care industry, and in food storage, environmental, and biomedical applications. Several reviews and book chapters have been dedicated in various areas of the application of AgNPs. Herein, we are interested in emphasizing the applications of AgNPs in various biological and biomedical applications, such as antibacterial, antifungal, antiviral, anti-inflammatory, anti-cancer, and anti-angiogenic. [24]

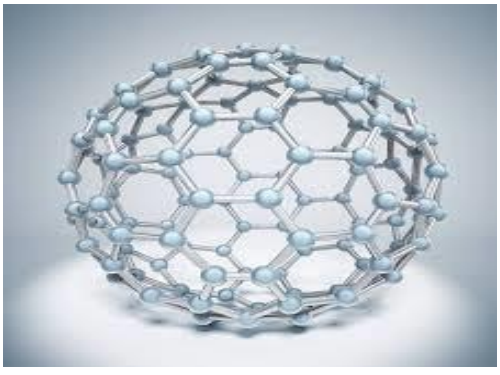

Fig 1.5 Structure of Silver Nanoparticle

OBJECTIVES OF THE PRESENT WORK

- To synthesis the silver nanoparticles (AgNPs) using (+)catechin-CT (flavanol)
- To investigate the binding mechanism of bioconjugated AgNPs-CT with BSA using spectroscopy and molecular docking method.
- To identify the binding pocket of BSA with the interaction of bioconjugation of AgNPs-CT using molecular docking studies.
- To evaluate the Biological activity of bioconjugated CT with AgNPs and BSA.

CHAPTER – II

REVIEW OF LITERATURE

2.1 Introduction

This chapter deals with the literature review on the interaction of Bovine Serum Albumin (BSA) with (+) catechin (CT) and Silver Nanopartiles (AgNPs) using Spectroscopy and molecular docking methods. Review of Literature is an important part of the project.

2.2 Overview of Literature

Anitha.S et al., (2022) studied the interaction of two stereoisomeric flavanols (+) catechin (CT) and (−) epicatechin (ECT) with bovine serum albumin (BSA) has been studied using UV–Vis absorption and fluorescence spectroscopy. The binding affinity between flavanols and BSA is investigated through fluorescence quenching. Fluorescence study showed that both flavanols exhibit a strong interaction with BSA at a single binding site. This investigation indicated that CT/ECT may quench BSA fluorescence by the static quenching process due to the formation of ground state complex. The binding pocket of BSA is identified at the site I/II with the interaction of CT/ECT using molecular docking studies. Molecular dynamics simulation (MDS) reported the structural changes of BSA into sturdy α-helix formations owing to the interaction of CT/ECT. During the 200 ns simulation, BSA-ECT complex had lower root mean square deviation values, and undergoes slight structural deformations. The MDS result shows that the binding of CT/ECT with BSA is due to hydrophobic and hydrogen bond interactions, which supports the experimental outcomes. The analysis of radius of gyration confirmed that the BSA-ECT complex possessed a more compact structure. CT and ECT differ in their binding site and structural effects caused by distinct orientational positions at the benzopyran moiety [42].

A.Kavitha, S.Ravichandran (2021) evaluated the antimicrobial and therapeutic properties of plant extracts and silver nanoparticles. The silver nitrate nanoparticles developed from plant extracts like Tulsi (Ocimum tenuiflorum), Spearmint (Mentha spicata), Neem (Azadirachta indica) (TSNLs) leaves have shown strong applications as the agent for stabilizing the TSNLs extracts. The maximum amounts of volatile compounds are present in the Beta-Caryophyllene, Carvone and Phytol of Tulsi, Spearmint and Neem extracts. Optimal extract absorption of the TSNLs extracts was determined in 0.03 mol/L, individually, with

0.951% yield recorded. The TEM analysis of silver nitrate nanoparticles were done in an average diameter of 10 nm. A crystal magnitude of 12 nm was considered in the XRD investigation. In the TSNLs leaf extracts at 92.1667 ± 0.3626%, FTIR analysis showed no chemical connections with the covering element. Escherichia coli and Staphylococcus aureus were employed to evaluate the antibacterial activities of the silver nanoparticles. In these samples, antimicrobial properties were evaluated in a gram negative and gram-positive microbes and fungal strains. The results showed that the nanoparticles made with TSNLs had produced quick natural control against pests and microbes, showed promising applications against pathogenic and spoilage microbes. The results also showed that these antimicrobial properties can be further improved through increasing the levels of the nanoparticle formulations [44].

SedighehHashemnia et al., (2021) examined the extensive application of AgNPs in medicine, the influence of AgNPs on the binding of clonazepam to BSA using Ultraviolet-Visible (UV–Vis), fluorescence, and circular dichroism (CD) spectroscopic methods. Detailed insights into the binding sites of clonazepam on the PVP-AgNP surface in the absence and presence of BSA have been obtained by carrying out molecular dynamics (MD) simulations and molecular docking analysis. UV–Vis results shown that the interaction between BSA and AgNPs causes formation of BSA-AgNP complexes. CD studies implied the formation of BSA-AgNPs complexes is accompanied by conformational changes in the secondary structural level of the protein. The intrinsic fluorescence of BSA solution in the simultaneous presence of AgNPss and clonazepam shown that clonazepam interacts considerably more with BSA-AgNPs complexes than with BSA. MD simulations results show that clonazepam molecules bind more to the PVP polymer film than to the bare Ag (0) atoms on the PVP-AgNPs surface. Molecular docking analysis shows a binding affinity of −19.77 kJ/mol for BSA-AgNPs complexes. Also, the results show that, although the IIA and IIIA domains in BSA play an important role in the docking of clonazepam with BSA, in BSA-AgNPs complexes, clonazepam molecules bind to the bare $Ag^{(0)}$ atoms, and there is also the possibility of interaction between PVP and BSA via clonazepam [43].

Sourav Das et al., (2020) reported the synthesis of AgNPs using green tea (GT) extract and two of its components, (-)-epigallocatechin gallate (EGCG) and CT as capping/stabilizing agents. The synthesized AgNPs showed antibacterial activity against the bacterial strains Staphylococcus aureus of and Escherichia coli, along with anticancer activity against HeLa cells. After administering nanoparticles to the body, they come in contact with proteins and

results in the formation of a protein corona (PC); hence they studied the interactions of these biocompatible AgNPs with hen egg white lysozyme (HEWL) as a carrier protein. Static quenching mechanism was accountable for the quenching of HEWL fluorescence by the AgNPs. The binding constant (Kb) was found to be higher for EGCG-AgNPs (2.309±0.018´104 M-1) than for GT-AgNPs and Ct-AgNPs towards HEWL. EGCG-AgNPs increased the polarity near the binding site while Ct-AgNPs caused the opposite effect, but GT-AgNPs had no such observable effects. Circular dichroism studies indicated that the AgNPs had no such appreciable impact on the secondary structure of HEWL. The key findings of this research relate to the synthesis of AgNPs using GT and its constituent polyphenols, and showed significant antibacterial, anticancer and protein-binding properties. The –OH groups of the polyphenols drive the in situ capping/stabilization of the AgNPs during synthesis, which might offer new opportunities having implications for nanomedicine and nanodiagnostics [41].

P.ChanphaiH, .A.Tajmir-Riahi (2019) determined the binding efficacy of tea catechins CT, (−)-epicatechin gallate (ECG) and (−)-epigallocatechin gallate (EGCG) with human serum albumin (HSA) and bovine serum albumin (BSA) in aqueous solution at physiological pH. Thermodynamic parameters ΔH^0 −13 to −8 (kJ mol^{-1}), ΔS^0 18 to 9 (J $mol^{-1}K^{-1}$) and ΔG^0 -14 to −13 (kJ mol^{-1}) showed tea catechins bind serum proteins via ionic interactions. The binding efficacy was 40–65% for polyphenol-protein conjugates. Modeling showed the presence of H-bonding, stabilizing catechin-protein conjugation with the free binding energy of −10.65 to −8.81 kcal/mol for catechin-HSA and −9.94 to −9.74 kcal/mol for CT-BSA conjugates. CT conjugation induced major perturbations of the protein conformation. Their studies indicated that serum proteins can transport tea CT in vitro [40].

KatarzynaRanoszek-Soliwoda, JaroslawGrobelny (2019) presented a synthesis protocol to obtain monodisperse AgNPs with plant extract. Cacao beans and grape seed extracts were selected as natural sources of polyphenols having biomedical importance (e.g. catechin, tannic acid, epicatechin gallate) and used to synthesise using a chemical reduction method. Syntheses were carried out with different molar ratios of reagents to find the best conditions for obtaining AgNPs that are homogeneous in size and shape. The colloids obtained were characterised with UV–Vis spectroscopy, scanning transmission electron microscopy (STEM) and dynamic light scattering (DLS). It was found that syntheses carried out only with plant extract resulted in unstable colloids containing polydisperse nanoparticles. Stable colloids containing spherical monomodal particles were obtained by the incorporation of sodium citrate as an additional reagent in the synthesis mixture. The results obtained clearly indicate the

crucial role of sodium citrate in the synthesis of spherical AgNPs of controlled size using plant extracts for biological applications [39].

Siddhant Jain & Mohan Singh Mehata (2017) examined the synthesis of silver nanoparticles (AgNPs) using leaf extracts of Ocimum Sanctum (Tulsi) and its derivative quercetin (flavonoid present in Tulsi) separately as precursors to investigate the role of biomolecules present in Tulsi in the formation of AgNPs from cationic silver under different physicochemical conditions such as pH, temperature, reaction time and reactants concentration. The size, shape, morphology, and stability of resultant AgNPs were investigated by optical spectroscopy (absorption, photoluminescence (PL), PL-lifetime and Fourier transform infrared), X-ray diffraction (XRD) analysis, and transmission electron microscopy (TEM). The enhanced antibacterial activity of AgNPs against E-Coli gram-negative bacterial strains was analyzed based on the zone of inhibition and minimal inhibitory concentration (MIC) indices. The results of different characterization techniques showed that AgNPs synthesized using both leaf extract and neat quercetin separately followed the same optical, morphological, and antibacterial characteristics, demonstrating that biomolecules (quercetin) present in Tulsi are mainly responsible for the reduction of metal ions to metal nanoparticles [38].

T. Fafal et al., (2017) investigated the phytosynthesis of AgNPs using an extract from the aerial parts of Asphodelus aestivus Brot. Ultraviolet–visible spectroscopy, fourier transform infrared spectroscopy (FT-IR), transmission electron microscopy (TEM) and zeta potential (ZP) were used to characterize the formation of silver nanoparticles (AgNPs). The antioxidant properties of these AgNPs were evaluated using DPPH, ABTS+ and hydrogen peroxide scavenging assays. The synthesized AgNPs were noticed through visual colour change from yellow to gray brown. The UV–Vis spectrum exhibited an absorption band at around 440 nm, which is a characteristic band for Ag. FT-IR measurement was carried out to identify the possible biomolecules responsible for capping and reducing agent for the Ag nanoparticles synthesized by A. aestivus aqueous extract. XRD results showed peaks at (200), (111), (110), (120), (330) and (210), which confirmed the presence of AgNPs with mono clinic crystals. The TEM image of silver nanoparticles shown that the morphology of silver nanoparticles was predominantly spherical. It could be concluded that A. aestivus extract can be used efficiently in the production of potential antioxidant AgNPs for commercial application [37].

Nada ShaeelAL-Thabaiti et al., (2017) investigated the interaction between BSA and AgNPs as a function of particle size and shape. UV–vis analysis implies the formation of the ground state complex between BSA and AgNPs through electrostatic interactions. The fluorescence spectra indicated that the AgNPs have a potent ability to quench the intrinsic fluorescence of BSA by static quenching mechanisms. The different parameters (the apparent association constant (K_{app} = 2.6 × 10^4 mol^{-1} dm^3), Stern–Volmer quenching constant (K_{SV} = 3.5 × 10^4 mol^{-1} dm^3), number of binding sites (n = 1.3) and bimolecular rate constant of the quenching reaction (k_q = 6.1 × 10^{12} mol^{-1} dm^3 s^{-1})) were calculated by using the UV–Vis and fluorescence spectra. The indole moieties of tryptophan residues of BSA were responsible to the complex formation with AgNPs in ground and excited states via electrostatic, van der Waals, hydrogen bonding, hydrophobic and hydrophilic interactions. Adsorption of AgNPs into the core of BSA changes the tryptophan environment from hydrophobic to hydrophilic (from folding to partially folded and/or unfolded). Circular dichroism results suggested that the helicity of BSA decreased from 67.68% to 60.25% and 67.68% to 45.42% with [AgNPs] and temperature [36].

MunevverSokmen et al., (2017) studied metallic AgNPs using green tea extract and microwave power. Two approaches were employed for AgNP production. Firstly, crude aqueous tea extract was filtrated and directly used in microwave assisted AgNP production system. Secondly, CT were selectively extracted from crude extract and 2% (w/v) aqueous solutions of CT extract has become available in the same process. A certain volume of extract (0.5 ml or 5 mL) was added to $AgNO_3$ solution (1–6 mM) and exposed to microwave radiation for 1, 5, 15 and 30 min in the presence and absence of capping agent polyethylene glycol (PEG). Plasmon resonance (SPR) absorption spectra were measured, thereby optimum conditions were determined. AgNPs were succesfully produced by both extracts only with 0.5 mL extract volume. Large volume of extract (5 mL) produced larger particles in all cases. CT extract was superior when compared with crude extract as the former produced high concentration of AgNPs at average 15 ± 6 nm particle size [35].

AdityBose (2016) investigated the interactions of tea polyphenols, namely (−) Catechin (C), (−)-epicatechin (EC), (–) epicatechin-3-gallate (ECG), (−)-epigallocatechin (EGC) and (−)-epigallocatechin-3-gallate (EGCG) with the serum albumin proteins. These interactions had all resulted in binding with the proteins with a concomitant static quenching of the protein fluorescence. A fluorescence technique is considered as the tool to comprehend the polyphenol–protein interactions mainly and simultaneously other spectroscopic techniques

used to verify the results. In this the different types of equations employed to calculate the binding constant values have been outlined, namely, modified Stern Volmer plot, Scatchard plot and Lineweaver Burk equation, with their corresponding results. The n values (number of binding sites) had always been close to unity suggesting a 1:1 complexation with the polyphenols and the protein. A structural change in the polyphenols has been found to alter the binding constant value and the galloyl moiety attached to the C ring of the polyphenols have been found to play a crucial role in this regard. It has been found that an increase in galloyl moiety increases binding of the CT with proteins [34].

P.Chowdhury et al., (2016) studied the synthesized green AgNPs with CT as reducing agent. CT, a polyphenol being itself having antiviral property may enhance the efficiency of AgNPs. They evaluated biogenic CT-AgNPs against Japanese encephalitis virus (JEV), which is a major public health problem particularly in Asia. Transmission Electron Microscopy (TEM) analysis revealed formation of biogenic AgNPs within the size of 50nm. Maximum (100%) cell viability for green nanoparticles was observed in the range from 0.04µg/ml to 5.85 µg/ml. Within the same range CPE inhibition assay also showed full protection against JEV. Further, virus yeild reduction assay showed reduction in plaques number in comparison to virus control in both pre & post JEV infection cells. This study demonstrated the ability of CT reduced biogenic AgNPs to prevent JEV infection by inhibition of virus attachment and post infection spread [33].

XiangrongL, iYongbingHao (2015) studied the interaction between CT and BSA was investigated using isothermal titration calorimetry (ITC), in combination with fluorescence spectroscopy, UV–Vis absorption spectroscopy, and Fourier transform infrared (FT-IR) spectroscopy. Thermodynamic investigations reveal that the electrostatic interaction and hydrophobic interaction are the major binding forces in the binding of CT to BSA. The binding of (+) CT to BSA is synergistically driven by enthalpy and entropy. Fluorescence experiments suggested that CT can quench the fluorescence of BSA through a static quenching mechanism. The obtained binding constants and the equilibrium fraction of unbound CT show that CT is stored and transported from the circulatory system to reach its target organ. Binding site I is founded as the primary binding site for CT. Additionally, as shown by the UV–Vis absorption, synchronous fluorescence spectroscopy and FT-IR, CT may induce conformational and micro environmental changes of BSA [32].

SaurabhGautam et al., (2013) investigated the formation and growth of hybrid nanoparticles of a protein BSA and silver by ultrasonic assistance and tracked by surface plasmon resonance signal of silver nanoparticles and light scattering. The hybrid nanoparticles were characterized by surface plasmon resonance spectra, light scattering, TEM, circular dichroism spectroscopy and zeta potential. Size along with the spherical shape of the nanoparticles could be controlled and nanoparticles with diameters ranging from 8 to 140 nm could be obtained, depending upon the ultrasonication time (15–30 min) and molar ratio of $AgNO_3$/BSA (20–200). The role of single free thiol group in the reduction of silver ions was also investigated by using DTNB modified BSA and protein conjugated silver nanoparticles were formed even with thiol modified BSA. The growth and size of the nanoparticles were governed by ultrasonic assisted Ostwald ripening. BSA conjugated with silver nanoparticles showed changes in the secondary structure with an increase in the beta sheet structure to 33% as compared to 7% in native BSA as determined by CD spectra. Zeta potential measurements in the pH range of 2.0–12.0 demonstrated that the surface charges of the BSA conjugated silver nanoparticles were similar to that of native BSA suggesting that surface charges and overall three dimensional structure of BSA did not change much. This approach provides a strategy for completely green synthesis of hybrid nanoparticles consisting of a biological entity and an inorganic material [31].

MihaelaSkrt, Natasa PoklarUlrih (2012) investigated the binding of several polyphenols to BSA at pH 7.5 and 25 °C: CT [(−)-epigallocatechin-3-gallate, (−)-epigallocatechin, (−)-epicatechin-3-gallate], flavones (kaempferol, kaempferol-3-glucoside, quercetin, naringenin) and hydroxycinnamic acids (rosmarinic acid, caffeic acid, p-coumaric acid). Fluorescence emission spectrometry and molecular docking were applied to compare experimentally determined binding parameters with molecular modelling. Among these polyphenols, (−)-epicatechin-3-gallate showed the highest Stern–Volmer modified quenching constant, followed by (−)-epigallocatechin-3-gallate. Similarly, (−)-epicatechin-3-gallate had the highest effect on the Circular Dichroic spectrum of BSA, while the changes induced by other polyphenols were negligible. Molecular docking predicted high binding energies for (−)-epicatechin-3-gallate and (−)-epigallocatechin-3-gallate for the binding site on BSA near Trp213. Their data reveals that the polyphenol structures significantly affect the binding process: the binding affinity generally decreases with glycosylation and reduced numbers of hydroxyl groups on the second aromatic ring [30].

Durba Roy et al., (2012) investigated the interactions of two stereoisomeric antioxidant flavonoids, CT and epicatechin (EC) with BSA and HSA, by steady state and time resolved fluorescence, phosphorescence, circular dichroism (CD), FTIR and protein–ligand docking studies. The steady-state fluorescence studies indicate a single binding site for both the ligands. FTIR spectra suggest that in both the albumins, CT and EC stabilize the α-helix at the cost of a corresponding loss in the β-sheet structure. CD studies have been carried out using CT, and both the epimers (+)CT and (−)C. The low temperature phosphorescence and protein–ligand [(+), (−) and (±) forms of C and EC] docking studies indicate that the ligands bind in the proximity of Trp 134 of BSA and Trp 214 of HSA, thereby changing their solvent accessible surface areas (ASA). Asn 158 and Glu 130 side chains are found to be within the hydrogen bonding distance from the phenolic –OH groups of CT and EC in the case of BSA complex. CT and EC are located within the binding pocket of sub-domain IIa of HAS [28].

MijunPeng et al., (2012) investigated the effect of heavy metal ions, Cd^{2+}, Hg^{2+} and Pb^{2+} on CT binding to BSA by spectroscopic methods. The results indicated that the presence of heavy metal ions significantly affected the binding modes and binding affinities of CT to BSA, and the effects depend on the types of heavy metal ion. One binding mode was found for CT with and without Cd^{2+}, while two binding modes – a weaker one at low concentration and a stronger one at high concentration were found for CT in the presence of Hg^{2+} and Pb^{2+}. The presence of Cd^{2+} decreased the binding affinities of CT for BSA by 20.5%. The presence of Hg^{2+} and Pb^{2+} decreased the binding affinity of CT for BSA by 8.9% and 26.7% in lower concentration, respectively, and increased the binding affinity of CT for BSA by 5.2% and 9.2% in higher concentration, respectively. The changed binding affinity and binding distance of CT for BSA in the presence of Cd^{2+}, Hg^{2+} and Pb^{2+} were mainly because of the conformational change of BSA induced by heavy metal ions [27].

AswathyRavindran, AmitavaMukherjee (2010) investigate the interaction between silver nanoparticles and BSA. The interaction of BSA [0.05–0.85% concentrations] with Ag nanoparticles [50 ppm concentration] in aqueous dispersion was studied through UV–vis spectral changes, morphological and surface structural changes. At pH 7, which is more than the isoelectric point of BSA, a decrease in absorbance at plasmon peak of uninteracted nanoparticles (425 nm) was noted till 0.45% BSA, beyond that a blue shift towards 410 nm was observed. The blue shift may be attributed to enhanced electron density on the particle surfaces. Increasing pH to 12 enhanced the blue shift further to 400 nm. The conformational changes in BSA at alkaline pH ranges and consequent hydrophobic interactions also played an

important role. The equilibrium adsorption data fitted better to Freundlich isotherm compared to Langmuir curve. The X-ray diffraction study revealed complete coverage of Ag nanoparticles by BSA. The scanning electron microscopic study of the interacted nanoparticles was also carried out to decipher morphological changes. This study established that tailoring the concentration of BSA and pH of the interaction it was possible to reduce aggregation of nanoparticles. Biofunctionalized AgNPs with reduced aggregation will be more amenable towards bio-sensing applications [26].

Athina Papadopoulou et.al (2005) studied the interaction between four flavonoids (catechin, epicatechin, rutin, and quercetin) and BSA was investigated using tryptophan fluorescence quenching. Quenching constants were determined using the Stern-Volmer equation to provide a measure of the binding affinity between the flavonoids and BSA. The binding affinity was strongest for quercetin and ranked in the order quercetin > rutin > epicatechin = catechin. The pH in the range of 5-7.4 does not affect significantly ($p < 0.05$) the association of rutin, epicatechin, and catechin with BSA, but quercetin exhibited a stronger affinity at pH 7.4 than at lower pH ($p < 0.05$). Quercetin has a total quenching effect on BSA tryptophan fluorescence at a molar ratio of 10:1 and rutin at approximately 25:1. However, epicatechin and catechin did not fully quench tryptophan fluorescence over the concentration range studied. Furthermore, the data suggested that the association between flavonoids and BSA did not change molecular conformation of BSA and that hydrogen bonding, ionic, and hydrophobic interaction are equally important driving forces for protein-flavonoid association.[25]

CHAPTER -III
METHODOLOGY

3.1 Introduction

Protein–ligand interaction is a subject of great interest in the biochemical field due to its scientific significance and practical applications in drug discovery [45]. Bovine serum albumin (BSA) has been extensively used to study the plasma protein binding ability of many ligands. It has a crystal structure similar to HSA, and is often used as a model protein instead of HAS [46]. The present study focuses the plasma protein binding interaction of BSA with (+) Catechin (CT) in presence of silver nanoparticle (AgNPs) using spectroscopic namely UV–Visible absorption, fluorescence spectroscopy and docking methods. These methods provide information about the binding mechanism and may evidence the conformational fluctuations of proteins in different environments. Fluorescence quenching is a method of determining the binding affinity of the fluorophores to quenchers [42]. Transmission Electron Microscope (TEM) analysis shows the structural characterisation of AgNPs.

3.2 Materials and Methods

3.2.1 Chemicals Used

Table 3.1 List of chemicals used in the experimental work

S.No	Chemicals Used	Chemical formula	Make
1	Bovine Serum Albumin		Sigma Aldrich
2	(+) Catechin hydrate	$C_{15}H_{14}O_{16}$	Sigma Aldrich
3	Silver Nitrate	$AgNO_3$	Hi-media

3.2.2 Stock Solutions

BSA stock solution (4×10^{-4} M) is prepared in Tris-HCl-NaCl buffer solution (pH = 7.4). BSA is dissolved in buffer in order to yield a solution with a concentration of 7×10^{-7} M for spectroscopic measurements. CT and $AgNO_3$ stock solutions is prepared in deionised water with a concentration of 0.17 mM and 1mM respectively.

3.2.3 Synthesis of the AgNPs

Silver nitrate ($AgNO_3$) solution was used for the synthesis of AgNPs. CT and $AgNO_3$ were prepared in deionized water. To form bioconjugate CTAgNPs, 5ml of CT (1mM) and 5ml of AgNO3 (0.6mM) solutions were mixed and stirred magnetically at 80 °C for 45 min. When the CT and $AgNO_3$ mixed with the deionized water, there is a colour change from colourless to pale yellow. The synthesized AgNPs were noticed through visual colour change. This color change indicates the formation of AgNPs in the solution. Figure 4.1 shows the colour change due to the formation of AgNPs. The synthesised AgNPs were characterized by UV-Vis absorbance spectroscopy and TEM. [47,51]

Fig 3.1 Synthesis of CT-AgNPs

3.3 Characterization of Techniques

The optical property and antioxidant activity of AgNPs and the bioconjugates were analysed in the region of 200-800 nm using V-670 UV-VIS NIR absorption spectrophotometer. Morphology is analysed using high resolution transmission electron microscopy (HRTEM, FEI-TECNAI T20 G2).

3.3.1 Optical Analysis

3.3.1.1 Ultraviolet–Visible (UV–Vis) Spectroscopy

UV-Vis spectroscopy is an analytical technique that measures the amount of discrete wavelengths of UV or visible light that are absorbed by or transmitted through a sample in comparison to a reference or blank sample. This property is influenced by the sample composition, potentially providing information on what is in the sample and at what concentration. To ascertain either AgNPs are developed or not visual and calorimetric appearance of samples checked by UV–Visible spectrophotometer before and after formulation of AgNPs at different time intervals. Electronic absorption spectra were recorded using UV–

Visible absorption spectrophotometer (V-670-Jasco) in the range of 200–800 nm. Distilled water was used as blank solution.

Light source

As a light-based technique, a steady source able to emit light across a wide range of wavelengths is essential. A single xenon lamp is commonly used as a high intensity light source for both UV and visible ranges. Xenon lamps are, however, associated with higher costs and are less stable in comparison to tungsten and halogen lamps.For instruments employing two lamps, a tungsten or halogen lamp is commonly used for visible light, whilst a deuterium lamp is the common source of UV light. As two different light sources are needed to scan both the UV and visible wavelengths, the light source in the instrument must switch during measurement.

Sample analysis

Whichever wavelength selector is used in the spectrophotometer, the light then passes through a sample. For all analyses, measuring a reference sample, often referred to as the "blank sample", such as a cuvette filled with a similar solvent used to prepare the sample, is imperative. If an aqueous buffered solution containing the sample is used for measurements, then the aqueous buffered solution without the substance of interest is used as the reference. When examining bacterial cultures, the sterile culture media would be used as the reference. The reference sample signal is then later used automatically by the instrument to help obtain the true absorbance values of the analytics. UV-Vis spectroscopy information may be presented as a graph of absorbance, optical density or transmittance as a function of wavelength. However, the information is more often presented as a graph of absorbance on the vertical y axis and wavelength on the horizontal x axis. This graph is typically referred to as an absorption spectrum. [48]

Fig 3.2 Ultraviolet–Visible Spectrometer

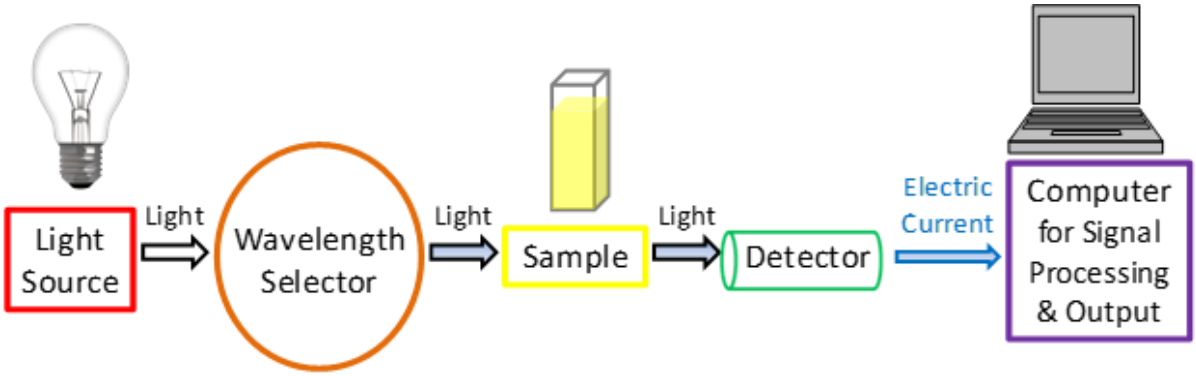

Figure 3.3: A simplified schematic of the main components in a UV-Vis spectrophotometer

3.3.1.2 Photoluminescence Spectroscopy

Photoluminescence spectroscopy, often referred to as PL, is when light energy, or photons, stimulate the emission of a photon from any matter. It is a non-contact, nondestructive method of probing materials. In essence, light is directed onto a sample, where it is absorbed and where a process called photo-excitation can occur. The photo-excitation causes the material to jump to a higher electronic state, and will then release energy, (photons) as it relaxes and returns to back to a lower energy level. The emission of light or luminescence through this process is photoluminescence, PL. Photoluminescence is when light energy, or photons, stimulate the emission of a photon. It takes on three forms: fluorescence, phosphorescence and chemiluminescence. Fluorescence is a type of luminescence caused by photons exciting a molecule, raising it to an electronic excited state. The excited state undergoes rapid thermal energy loss to the environment through vibrations, and then a photon is emitted from the lowest-lying singlet excited state. This process of photon emission competes for other non-radioactive processes including energy transfer and heat loss. Fluorescence emission measurements were performed on a RF-5301PC spectrofluorimeter (Shimadzu) equipped with a 150 W Xenon lamp. The fluorescence spectra were recorded with excitation wavelength at 278 nm and 3 nm/3 nm slit widths.

To determine the linear concentration range for protein fluorescence, a series of BSA solutions with increasing concentrations (0-26 *í*M) were prepared in buffer. The maximum excitation wavelength (*ì*ex) and maximum emission wavelength (*ì*em) for BSA were 282 and 348 nm, respectively. Therefore, 4×10^{-6} M BSA was chosen as the concentration for fluorescence quenching experiments. For each data point, 2 µL of the appropriate flavonoid solution (Pure CT, CT-AgNPS, CT Buffer) was added into 3 mL BSA solution, to give a final

flavonoid concentration. The change in fluorescence emission intensity was measured within 1 min of adding flavonoid to the BSA.

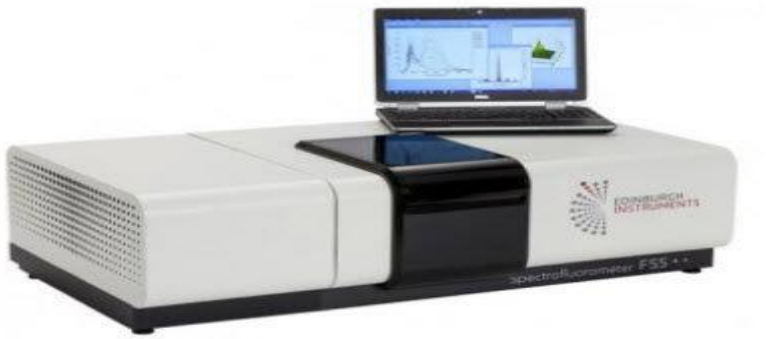

Fig 3.4 Photoluminescence Spectrometer

3.3.2 Morphological Analysis

3.3.2.1 TEM Analysis

The Transmission Electron Microscope (TEM) operates on many of the same optical principles as the light microscope. The TEM has the added advantage of greater resolution. This increased resolution allows us to study ultrastructure of organelles, viruses and macromolecules. Specially prepared materials samples may also be viewed in the TEM. The light microscope and TEM are commonly used in conjunction with each other to complement a research project.**TEM,** type of electron microscope that has three essential systems:

(1) an electron gun, which produces the electron beam, and the condenser system, which focuses the beam onto the object,

(2) the image-producing system, consisting of the objective lens, movable specimen stage, and intermediate and projector lenses, which focus the electrons passing through the specimen to form a real, highly magnified image, and

(3) the image-recording system, which converts the electron image into some form perceptible to the human eye. The image-recording system usually consists of a fluorescent screen for viewing and focusing the image and a digital camera for permanent records. In addition, a vacuum system, consisting of pumps and their associated gauges and valves, and power supplies are required.

Working

TEMs employ a high voltage electron beam in order to create an image. An electron gun at the top of a TEM emits electrons that travel through the microscope's vacuum tube. Rather than having a glass lens focusing the light (as in the case of light microscopes), the TEM employs an electromagnetic lens which focuses the electrons into a very fine beam. This beam then passes through the specimen, which is very thin, and the electrons either scatter or hit a fluorescent screen at the bottom of the microscope. An image of the specimen with its assorted parts shown in different shades according to its density appears on the screen. This image can be then studied directly within the TEM or photographed. Figure 1 shows a diagram of a TEM and its basic parts.

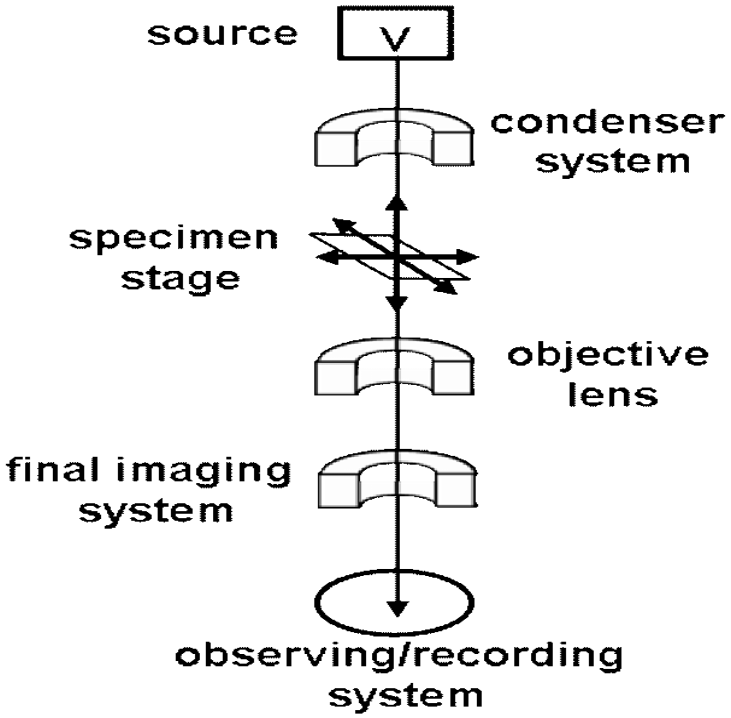

Fig 3.5 A schematic view of the fundamental components of a TEM instrument

Image recording

The electron image is monochromatic and must be made visible to the eye either by allowing the electrons to fall on a fluorescent screen fitted at the base of the microscope column or by capturing the image digitally for display on a computer monitor. Computerized images

are stored in a format such as TIFF or JPEG and can be analysed or image-processed prior to publication. The identification of specific areas of an image, or pixels with specified characteristics, allows spurious colours to be added to a monochrome image. This can be an aid to visual interpretation and teaching and can create a visually attractive picture from the raw image. It is mainly used to study surface morphology of synthesized AgNPs. TEM plates were prepared by addition of silver nitrate to develop smear of solution on slides.

Advantages of the Transmission Electron Microscope

Both the optical microscope and transmission electron microscope use thinly sliced samples. The advantage of the transmission electron microscope is that it magnifies specimens to a much higher degree than an optical microscope. Magnification of 10,000 times or more is possible, which allows scientists to see extremely small structures. For biologists, the interior workings of cells, such as mitochondria and organelles, are clearly visible. The transmission electron microscope offers excellent resolution of the crystallographic structure of specimens, and can even show the arrangement of atoms within a sample.

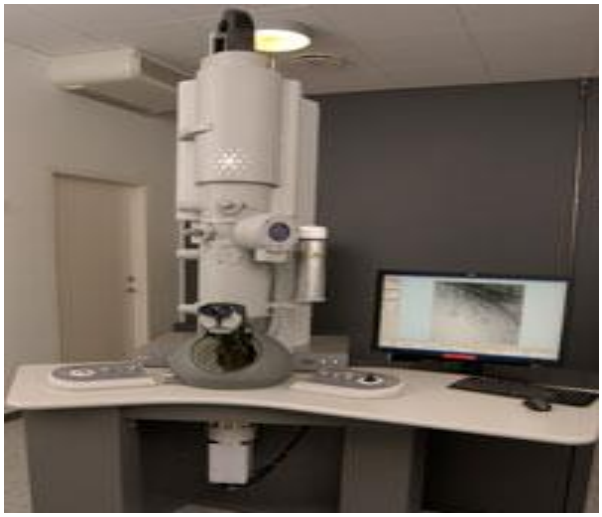

Fig 3.6 Transmission Electron Microscope

3.3.3 Antibacterial activity

Silver nano particles are one of the most attractive nonmaterial's for commercialization applications. As antibacterial agents silver nanoparticles were used for wide range of applications from disinfecting medical devices and home appliances to water treatment. AgNPs

promisingly used in drastic fields such as healthcare products, food storage, textile and medicinal devices. In antibacterial potential AgNPs free silver ions are released at slower rate along with higher surface area which produces noxious environment and this is the main reason for broad spectrum antibacterial potential of AgNPs

The antibacterial activity of pure CT and bioconjugation of AgNPs with CT (by both methods) is performed by Agar well diffusion method using Muller-Hinton Agar as growth media. The bacterial strains namely *Staphylococcus aureus* (*Gram-positive*) and *Pseudomonas aeruginosa* (*Gram-negative*) are used in this study. Sterile agar plates were inoculated and 20µl of pure CT, bioconjugates BSA-CT, BSA-CT AgNPs, CT-AgNPs were added separately into the wells bored in the agar medium. Then the plates were incubated at 37ºC for 24hrs. A well loaded with Ciprofloxacin served as positive control and was maintained on each plate.

3.4 Theoretical Methods

Computational docking is widely used for the study of protein-ligand interactions and for drug discovery and development. Docking is then used to predict the bound conformation and binding free energy of small molecules to the target. Single docking experiments are useful for exploring the function of the target, and virtual screening, where a large library of compounds are docked and ranked, may be used to identify new inhibitors for drug development. AutoDock is a suite of free open–source software for the computational docking and virtual screening of small molecules to macromolecular receptors. AutoDock/Vina was employed for docking using protein and ligand information along with grid box properties in the configuration file. The pose with lowest energy of binding or binding affinity was extracted and aligned with receptor structure for further analysis. Molecular docking is one of the most applied virtual screening methods, especially, when the 3D structure of target protein is available. This method could predict both the binding affinity between ligand and protein and the structure of protein–ligand complex, which is useful information for lead optimization. Indeed, molecular docking has been applied for more than three decades and a great number of new drugs have been discovered and developed accordingly. In order to make optimal use of limited computational resources, various scoring functions were developed for molecular docking to rapidly predict how strong the binding is between a chemical compound and a target protein/macromolecule.

3.4.1 Methodology of Docking

There are three important parts in this research. The first part is preparation of target protein and ligands, the second is running the molecular docking simulation, and the last part is data analysis.

The molecular docking procedure consist of the following

- Protein preparation
- Ligand preparation
- Receptor grid preparation
- Ligand docking preparation

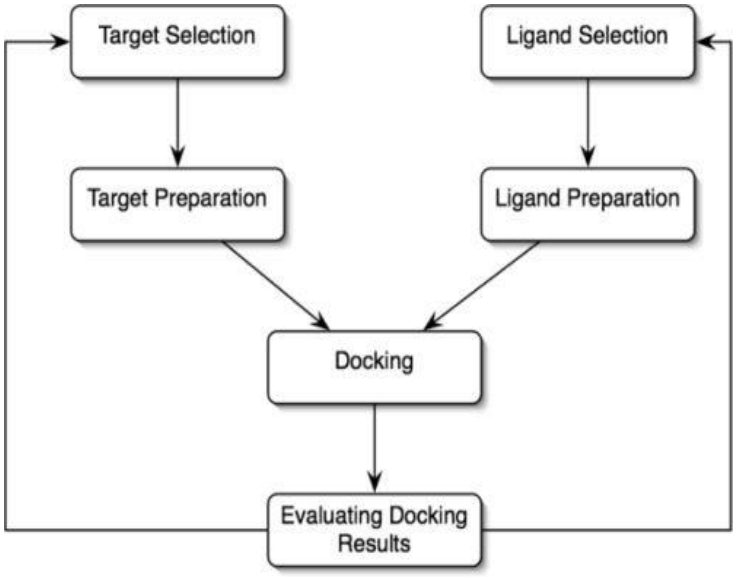

Fig 3.7 Protocol for using Molecular Docking

The monomer BSA crystal structure was taken from the Protein Databank (PDB ID:3V03), and the flavanols (CT and ECT) were used for molecular docking studies. Using the DelWaterObj and DelMol tools, the protein is pre-processed by eliminating the water molecules and co-crystallized flavanols from the coordinate system. The polar hydrogen atoms were then added to the pre-processed protein according to fundamental chemistry principles and the bond sequences were altered using the AddHyd command. Almost 10 independent docking runs were performed, and minimum energy conformers were saved for each complex. AutoDock Vina performed the computation of grid maps and grouping of dock results automatically[43]. LigPlot+ is applied to find the configuration of hydrophobic interaction of the amino acid residues of BSA with CT/ECT [42]

CHAPTER -IV
RESULTS AND DISCUSSION

4.1 Introduction

This study focuses on understanding the interaction of biosynthesized silver nanoparticle (AgNPs) using (+) Catechin (CT) with Bovine Serum Albumin (BSA) by different types of spectroscopic techniques. The binding characteristics of the interaction between the CT-AgNPs and BSA were explored by UV-Vis Spectroscopy. The structural characterization of biosynthesized AgNPs was confirmed by Transmission Electron Spectroscopy (TEM). The synthesized AgNPs with BSA and CT showed the enhanced antibacterial activity against the bacterial strains. Fluorescence results suggested the contribution of static quenching in the complex formation between CT-AgNPs and BSA. The binding pockets of CT-AgNPs and CT with BSA were identified using molecular docking methods.

4.2 Analysis of formation of Silver Nanoparticle

4.2.1 UV-Vis Spectral analysis of AgNPs

UV-Vis Spectroscopy was used to do preliminary characterisation of the AgNPs. To assess the stability of silver nanoparticles, UV-Vis Spectroscopy was used to examine the generated AgNPs during a 10-day period [54]. The bioreduction ability of CT from Ag^{+} to Ag^{0} is indicated by their absorption maxima at 395nm. The UV-Vis spectrum of bioconjugates show a peak at 278 nm, which can be attributed to the presence of pure CT molecules [42]. Even after 10 days, the silver nanoparticles exhibited the same peak at the same wavelength with the same absorption intensity as seen in Fig 4.1. The colloidal mixture was found to be stable for 10 days, which was very helpful and convenient for nanoparticle manufacturing. [54].

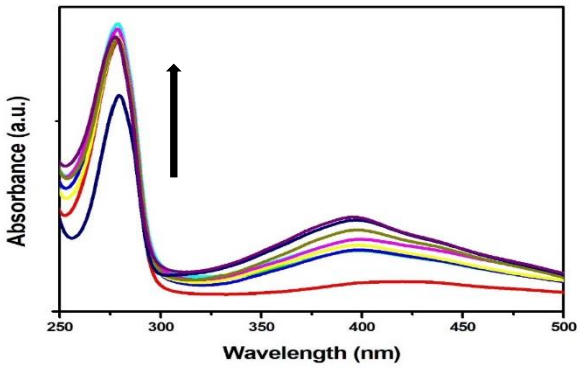

Fig 4.1 UV-Vis absorption spectra of AgNPs synthesized by using CT

4.2.2 TEM Analysis

TEM analysis was carried out for the determination of morphology, size of the synthesized AgNPs. Fig 4.2 shows the TEM image of synthesized AgNPs by CT. The TEM image and size distributions of Ag-NPs showed that the mean diameter of the AgNPs ranged from about 20 to 50 nm. TEM analysis indicated that the synthesized AgNPs using CT extract were observed to be uniform and mostly spherical in shape. CT significant role in the reduction of Ag^{+} ions, as stabilizing or capping agents in the synthesis of AgNPs, and may therefore have an effect on the morphology of biocompatible AgNPs. The selected area of electron diffraction pattern indicated that the AgNPs are crystalline in nature, and the bright circular rings signify the presence of different AgNPs planes as shown in Fig 4.2 (c).

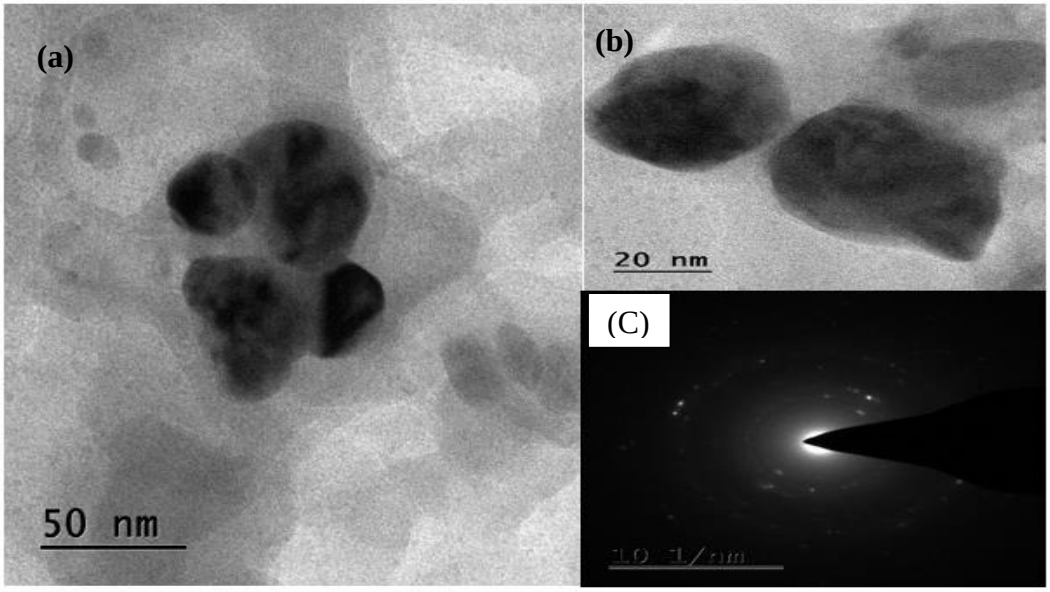

Fig 4.2 TEM image (a) 50nm (b) 20nm and (c) SAED pattern of AgNPs-CT

4.3 Interaction of CT-AgNPs with BSA

4.3.1 UV-Vis absorption spectral analysis of CT and CT-AgNPs with BSA

UV-Vis absorption spectral studies are used to examine the formation and conformational fluctuations of BSA protein interacted CT complexes. The UV-Vis absorption spectra of the complexes BSA-CT are shown in Fig. 4.3 a. The concentration of BSA in buffer is fixed at 7×10^{-7}M. The CT (0.17m) of 2µl is titrated step by step into BSA, hence the concentration varies from 1.4×10^{-7}M to 1.4×10^{-6}M. The total accumulated volume of titrated antioxidant solution is 20µl [52]. The UV-Vis absorption spectrum of BSA shows two

characteristic absorption peaks in the region of 200 to 300nm; one strong absorption peak at 203nm is due to BSA framework, while another absorption maxima appearing at 280nm may be due to tryptophan, tyrosine and phenylalanine amino acids [54]. The optical absorbance at 280nm and 203nm increases with increasing the concentration of CT in BSA.

The UV-Vis absorption spectroscopy is the most reliable technique for the study of protein interaction with metal nanoparticles. To examine the impact of bioconjugation on the absorption spectra of BSA and CT-AgNPs, the UV-Vis absorption spectra of native BSA at various concentrations of CT-AgNPs were taken and obtained absorption spectra are shown in Fig. 4.3 b. The concentration of BSA in buffer is fixed at 7×10^{-7}M. The CT-AgNPs of 2µl is titrated step by step into BSA so that the concentration varies from 1.4×10^{-7}M to 1.4×10^{-6}M. The total accumulated volume of titrated antioxidant solution is 20µl. The absorption spectra of the native form of BSA show an absorption band at 202 nm which arises due to BSA frame while another absorption maxima observed at 278 nm is due to the presence of aromatic amino acid residues (tryptophan and tyrosine) and disulfide bond [49]. It is observed that the absorbance increases regularly on increasing the concentration of CT-AgNPs. The results obtained from the absorption spectra revealed the complex formation between BSA and CT-AgNPs [54]. With the increasing concentration of CT-AgNPs, there is a gradual increase in absorption intensity, indicating the complex formation between the BSA and CT-AgNPs. However, there are possibilities of hydrophobic interactions playing a crucial role in the bio-conjugation of CT-AgNPs with BSA. The results obtained from UV-Vis spectral investigation are in good agreement with the reported literature about the conjugation of protein with nanoparticles [55].

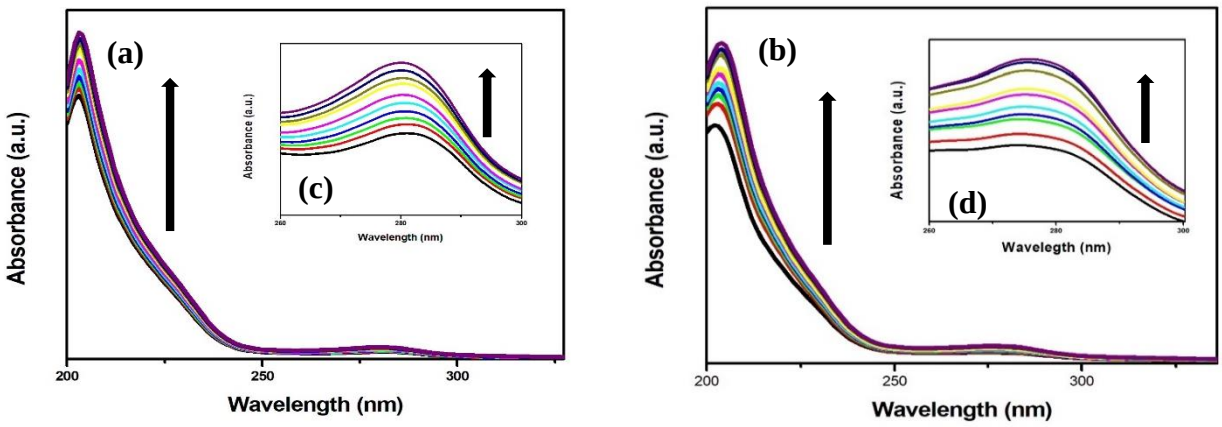

Fig. 4.3.UV-Vis absorption spectra of BSA ($7x10^{-7}$ M) with (a) CT and (b) CT-AgNPs varies from 0,$1.4 x 10^{-7}$M to $1.4 x 10^{-6}$M (inset c,d enlarged region from 260 nm to 300nm)

4.3.2 Fluorescence quenching of BSA by CT and CT-AgNPs

The most reliable and commonly used technique for studying protein-ligand and protein nanoparticle interactions is fluorescence spectroscopy. Fluorescence emission spectral analysis was performed to check the effect of CT-AgNPs and CT on the fluorescence emission intensity of BSA. The fluorescence quenching spectra of BSA in the presence of the varying concentration of CT and CT-AgNPs are shown in Fig. 4.4 a and b. From Fig 4.4 a, the fluorescence spectrum of BSA is found to have emission maximum at 353 nm with an excitation wavelength of 278 nm, which is mainly attributed to emission of tryptophan, tyrosine and phenylalanine residues [56]. It is seen that fluorescence intensity of BSA decreases with increase in the concentration of CT. The progressive quenching in fluorescence intensity shows the formation of a complex between BSA and CT [49]. It indicates that the CT can interact with BSA and quench the intrinsic fluorescence of BSA. The result suggests that the fluorophores of BSA is quenched with the possibility of hydrophobic and electrostatic interactions. The hydrophobic interaction may arises due to the changes in the microenvironment of the BSA residues [42].

The fluorescence spectrum of BSA –CT-AgNPs is found to have emission maximum at 360 nm with an excitation wavelength of 278 nm. A blue shift of 2nm in fluorescence emission of BSA was seen with an increasing concentration of CT-AgNPs which is shown in Fig 4.2b. The blue shift showed that the increase in hydrophilicity and polarity around the fluorophore regions. The fluorescence quenching may be categorized into dynamics and static mechanisms; the former involves the collision between fluorophore and quencher in the excited state of fluorophore while the latter is an outcome of the ground state fluorophore-quencher complex formation [57]

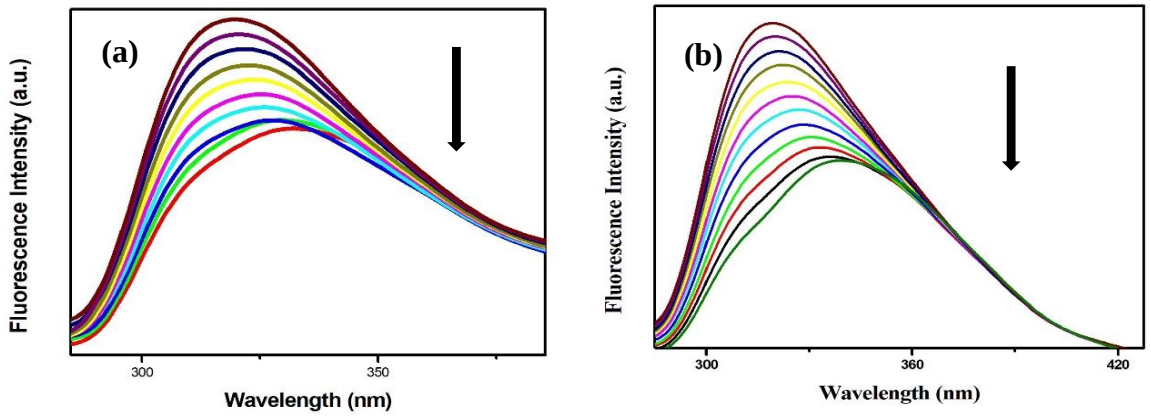

Fig 4.4 Variation in the intrinsic fluorescence of BSA on interaction with (a) CT and (b) AgNPs with CT

The Stern-Volmer quenching constant (*Ksv*) and different parameters of the quenching mechanism were calculated by the following equation

$$F_O/F = 1 + K_{sv}[Q] \qquad (1)$$

Where *F0* and *F* are the fluorescence intensities of quencher in the absence and presence of quencher respectively, *Ksv* is the Stern-Volmer constant, [Q] is the concentration of quencher, kq is the quenching rate constant and τo is the average fluorescence lifetime of protein fluorophores in the absence of a quencher. Fig.4.5 represents the Stern-Volmer plot, between F0/F versus [Q] [49]. The obtained K_{sv} value from the slope of F0/F versus [Q] with interaction of CT-AgNPs is $1.31\times10^4\ M^{-1}$ and CT is $0.862\times10^4\ M^{-1}$ with $R^2 = 0.9985$ and $R^2 = 0.9953$. The resulting plot exhibits a good linearity. It indicates that either static or dynamic quenching plays a major role in the quenching process.

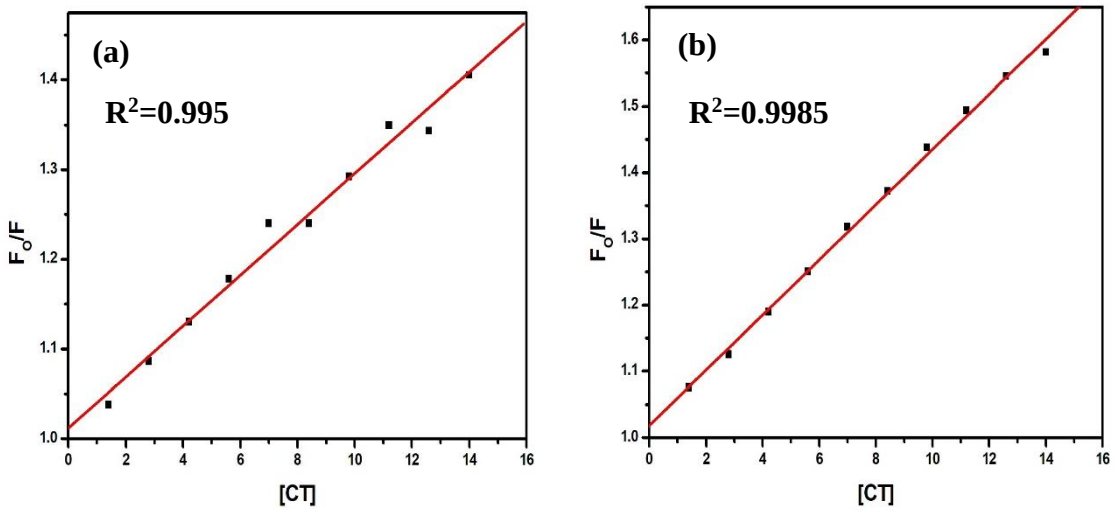

Fig.4.5 Stern-Volmer plot for BSA with (a) CT and (b) CT-AgNPs

The possibility of static or dynamic quenching is verified by calculating bimolecular quenching rate constant (k_q) using the following equation

$$\frac{F_0}{F} = 1 + k_q \tau_0 [Q] \qquad (2)$$

τ_0 is the life time of the BSA fluorophores which is about 6×10^{-8}s [42]. From the obtained K_{sv} value, the calculated K_q value is 2.183×10^{11} M^{-1} S^{-1} for BSA with CT-AgNPs and 1.438×10^{11} M^{-1} S^{-1} for CT. The obtained K_q value is greater than 2×10^{10} M^{-1} S^{-1} which suggest that the complexation of BSA with biocompatible AgNPs and CT takes place through a static quenching mechanism.

4.3.2.1 Binding parameters of BSA-CT-AgNPs and BSA-CT complexes

The binding parameters are important to study pharmacodynamics and pharmacokinetics. When a small molecule binds independently to a set of homologous sites on a large molecule, the convergence between the free molecule and the binding molecule is calculated by the following equation

$$\log_{10}\left[\frac{F_0 - F}{F}\right] = \log_{10} K_a + n \log_{10}[Q] \qquad (3)$$

where, K_a is the apparent binding constant to a site, and n is the number of binding sites per BSA. By the linear plot of $\log_{10}[(F_0\text{-}F)/F]$ versus $\log_{10}[Q]$, n and K_a can be obtained from the intercept and slope of the plot for the interaction of BSA with CT-AgNPs and CT, as shown in Fig 4.6 respectively [42]. For positive cooperativity, n >1, which signifies that the adsorption of a BSA molecule on the nanoparticle surface enhances the attachment of other protein units to the same surface. In contrast, for negative cooperativity, n < 1, which means that when additional BSA are adsorbed to the surface, the binding affinity of the BSA is gradually decreases and n = 1 reflects non-cooperative interactions where the resulting binding of BSA is independent of the proteins already bound to the surface [41]. The binding constant and the number of binding sites are found to be $K_a = 3.841 \times 10^4$ L mol^{-1}, n = 1.01 for CT-AgNPs and for CT, $K_a = 2.112 \times 10^4$ L mol^{-1}, n = 0.92 (n<1). This indicates that binding of CT/CT-AgNPs occurs at only one site of BSA with 1:1.

The spontaneity of the association of the AgNPs with BSA was evaluated using the following Gibb's equation

$$\Delta G = -2.303\ 67\ RT \log K_a \qquad (4)$$

The obtained Gibb's free energy for CT-AgNPs with BSA is -26.7830 kJ/mol and for CT is -25.268 kJ/mol. The negative Δ*G* values for the complexation of the CT-AgNPs with BSA indicate the spontaneity of the interaction process.

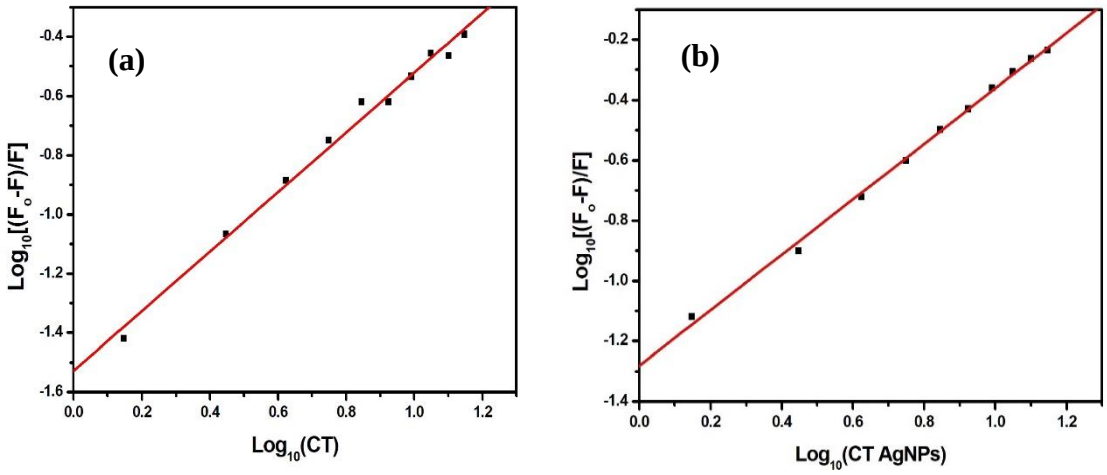

Fig 4.6 Stern-Volmer plot for $\log_{10}$ [(F_O-F)/F] versus (a) CT and (b) CT-AgNPs

Table 4.1. Binding parameters obtained for the interaction of BSA with CT-AgNPs

Complex	K_{SV} (10^4, M^{-1})	k_q (10^{11}, M^{-1} s^{-1})	K_a (10^4, M^{-1})	N	Δ*G* (kJ/mol)
BSA-CT	0.862	1.438	2.112	0.92	-25.268
BSA-CT-AgNPs	1.31	2.183	3.841	1.01	-26.7830

4.3.3 Antibacterial Activity

The nano dimension of AgNPs means that they have a higher surface-to-volume ratio relative to their bulk counterparts. This property of AgNPs facilitates their interaction with bacterial surfaces, which enhances the anti-bacterial propensity of AgNPs. By monitoring the zone of inhibition, the well diffusion method was used to investigate the antibacterial impact of AgNPs against *Staphylococcus aureus* (*S.aureus*) *(Gram-positive) and Pseudomonas aeruginosa* (*P.aeruginosa*) *(Gram-negative)* bacterial strains which is shown in Fig 4.7. The diameter of the inhibition zones is measured and tabulated in Table 4.2. The release of Ag^+ ions from AgNPs to bacterial cells is responsible for the improved bactericidal impact of AgNPs (20). The zone of inhibition of BSA-CT-AgNPs is 19mm, BSA-CTmm is 14mm, CT-AgNPs is 13mm and CT is 12mm against *S.aureus* and against *P.aeruginosa* the BSA-CT is

15mm, BSA-CT-AgNPs is 21mm, CT-AgNPs is 14mm and CT is 11mm. The maximum zone of inhibition of 19 mm was found at BSA-CT-AgNPs against *S. aureus* and 21 mm against *P.ae*ruginosa . From Table 4.2 and Fig. 4.7, it can be seen that BSA-Ct-AgNPs showed enhanced anti-bacterial effects (growth inhibition is confirmed by the clear inhibitory zones) against both *S.aureus* and *P.aeruginosa* as compared with samples BSA-CT, CT-AgNPs and CT as depicted in Fig. 4.7

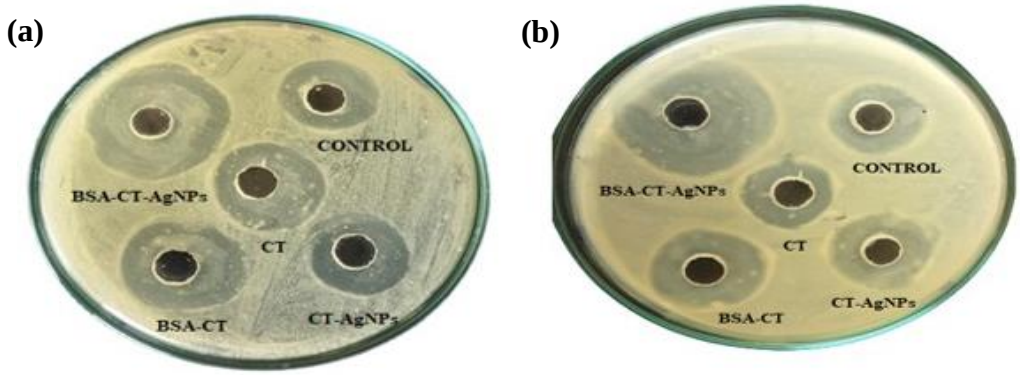

Fig 4.7 Antibacterial efficiency of BSA-CtAgNPs, CT-AgNPs, BSA-CT and CT against (a) *Staphylococcus aureus* and (b) *Pseudomonas aeruginosa*

Table 4.2. Zone of inhibition of the bacterial strains in the presence of the respective AgNPs (20 μg/ mL).

Compound	***Staphylococcus aureus*** **(mm)**	***Pseudomonas aeruginosa*** **(mm)**
BSA-CT-AgNPs	19	21
BSA-CT	14	15
CT-AgNPs	13	14
CT	11	12

4.4 Molecular docking

Molecular docking is an effective In silico method implemented to identify the protein-ligand with metal nanoparticles binding site and obtain the binding affinity of the binding site. The structure of BSA is made up of three homologous α-helical domains I, II and III, each domain is constituted by two subdomains A and B. The blind docking confirmed that the binding site is identified in subdomain IIIA at sudlow site II for BSA- CT interaction and for

CT-AgNPs interaction the binding site is identified at subdomain IA. The molecular docking conformations of BSA-CT/CTAgNPs with lowest binding energy are presented in the Fig.4.8 a and 4.8 b respectively. The binding affinity of BSA-CT and BSA-CTAgNPs has been found to be -7.9 kcal/mol -2.8 kcal/mol. During the interaction, the amino acids residues that surrounding CT in the binding site were Arg458, Leu189, His145, Thr190, Ser192, Ser428, the residues involved in the interaction of CT-AgNPs of BSA are Lys20, Leu24.

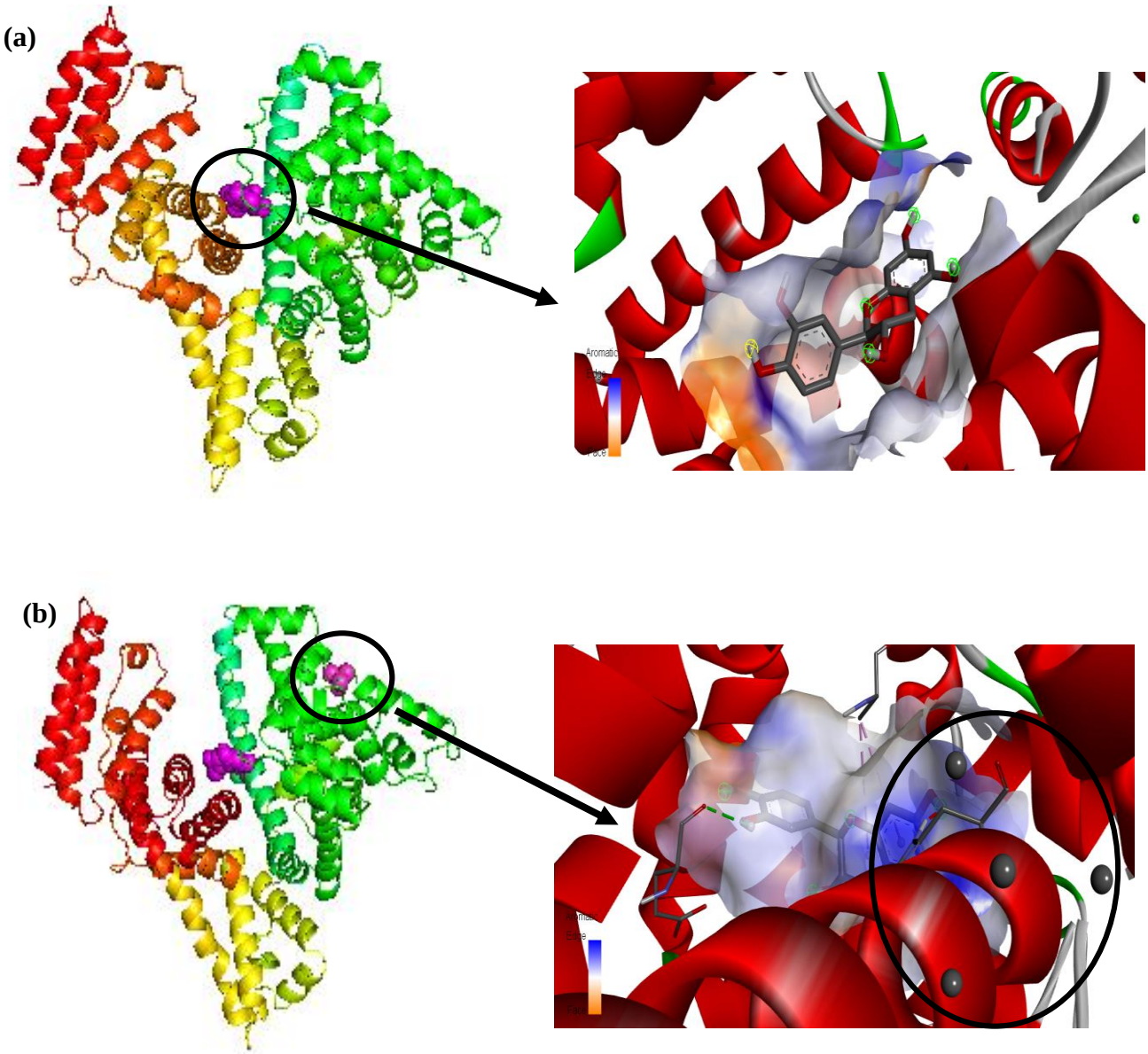

Fig 4.8 The molecular docking confirmation of (a) BSA-CT and (b) BSA-CT-AgNPs complex with high binding affinity

The binding of CT/CT-AgNPS with BSA protein occurs by hydrogen bond interaction through hydroxyl groups of CT/CT-AgNPs and polar residues of BSA, as well as hydrophobic interaction between CT/CT-AgNPs planar ring surfaces and non-polar residues of BSA. The interaction plot produced by Ligplots given in Fig.4.9a and 4.9b show the possible hydrophobic interaction between residues of BSA and CT/CT-AgNPs and also shows the hydrogen bond length. From the Fig. 4.9a, the red arcs labelled with hydrophobic residues of BSA encircled by CT at site II are Lys211, Val215, Asp323, Leu326, Gly327 and Leu330. The hydrophobic interacting residues labelled in red arcs surrounded by CT-AgNPs are Ala193, Arg458, Tyr451, Leu189, Thr190 and Glu424 shown in Fig.4.9b. CT bound to BSA showed considerably high number of hydrophobic contacts than CT-AgNPs.

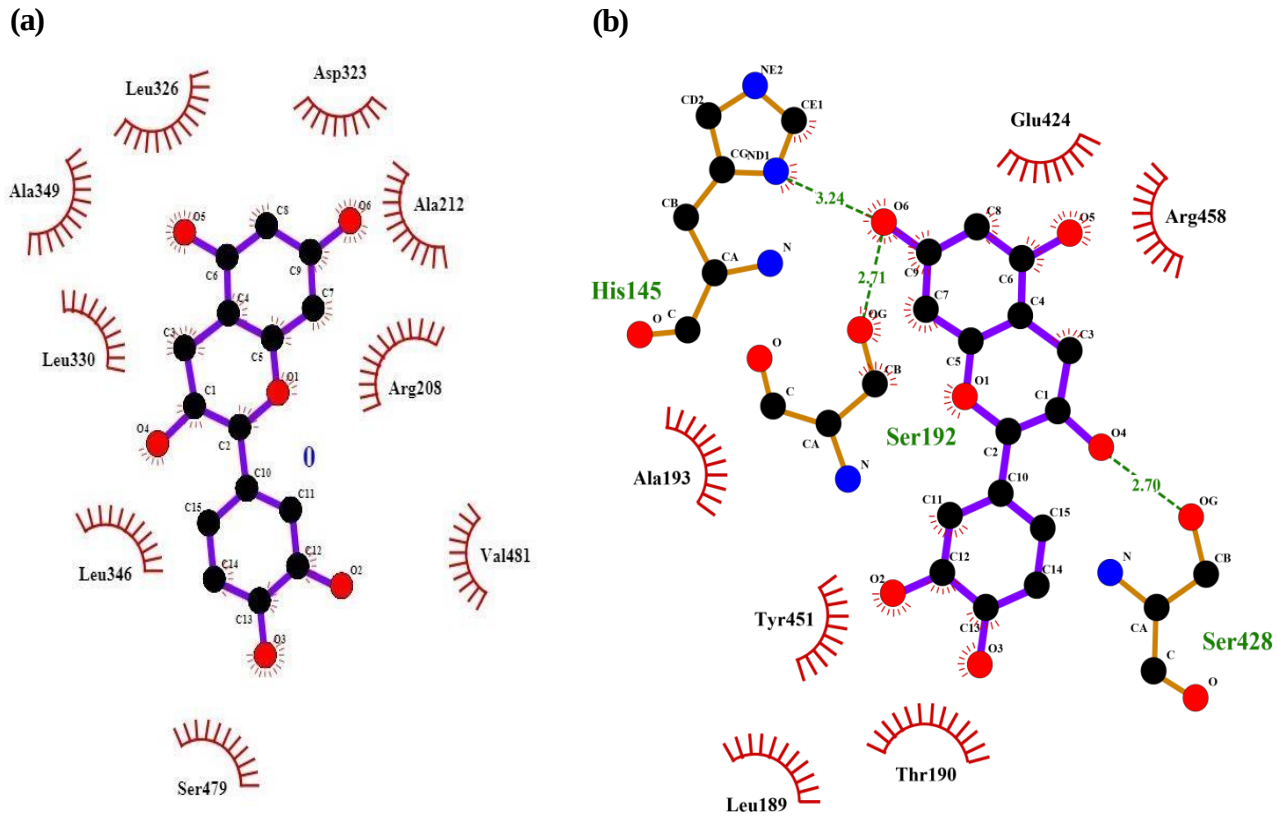

Fig.4.9 Two dimensional representations of ligplot of hydrophobic interaction residues of BSA with (a) CT and (b) CT-AgNPs

CHAPTER V

SUMMARY AND CONCLUSION

In the present study, the silver nanoparticle (AgNPs) was synthesized by (+) Catechin (CT). The formation of AgNPs was observed by the colour change from colourless to pale yellow and it was confirmed by UV-Vis spectroscopy and TEM. TEM studies revealed that the spherical shaped nanoparticles were in the range of 20-50nm. The binding mechanism of the interaction of flavanols CT and CT-AgNPs with BSA protein has been investigated using spectroscopic techniques. UV-Vis absorption spectra studies shows that there are possibilities of hydrophobic interactions playing a crucial role in the bio-conjugation of CT-AgNPs with BSA. According to fluorescence spectra, CT/CT-AgNPs interacts with BSA and quenches its intrinsic fluorescence via a static quenching mechanism and the values obtained for CT/CT-AgNPs is k_{sv}=.862×10^4 M^{-1} and 1.31×10^4 M^{-1}, K_q=1.438×10^{11} M^{-1} s^{-1} and 2.183×10^{11} M^{-1} s^{-1}, K_a = 2.112×10^4 L mol^{-1} and 3.841 ×10^4 L mol^{-1}, n = 0.92 and 1.01. This indicates that binding of CT/CT-AgNPs occurs at only one site of BSA with 1:1. The negative Δ*G* values for the complexation of the CT-AgNPs with BSA individually indicate the spontaneity of the interaction process. The interaction of BSA with CT-AgNPs enhanced antimicrobial efficacy against *Pseudomonas aeruginosa* than *Staphylococcus aureus.* Molecular docking study confirms that the binding of CT/CT-AgNPs occurs in the sudlow site of II with subdomain IIIA/IA of BSA.

REFERENCES

[1]. Tamara Topala, Andreea Bodoki, Luminiţa Oprean, and Radu Oprean. "Bovine Serum Albumin Interactions with Metal Complexes". Clujul Medical vol.84(4):215-219 (2014)

[2]. Tanveer A. Wani, Ahmed H. Bakheit, M. A. Abounassif and Seema Zargar. "Study of Interactions of an Anticancer Drug Neratinib with Bovine Serum Albumin: Spectroscopic and Molecular Docking Approach". Analytical Chemistry vol.6(2018)

[3]. Thomas E. Hamilton, John L. Rombeau, "Current Therapy in Colon and Rectal Surgery (Second Edition)", Nutritional Support (2005)

[4]. Michael A. Gropper, "Miller's Anesthesia, Hepatic Physiology, Pathophysiology, and Anesthetic Considerations" (Ninth Edition) (2020)

[5]. William Stillwell. "An Introduction to Biological Membranes ," Membrane Biogenesis (Second Edition) (2016)

[6]. David B.Reuben. "Nutritional Support for the Older Cancer Patient (Chapter -20)", Management of Cancer in the Older Patient vol.31:598-602 (2012)

[7]. lois MS., "Antioxidant determinations by the use of a stable free radical". Nature. (1998).

[8]. M.S. Brewer, Natural Antioxidants: Sources, Compounds, Mechanisms of Action, and Potential Applications, Food science, (2011).

[9]. Kanti Bhooshan Pandey and Syed Ibrahim Rizvi "Plant polyphenols as dietary antioxidants in human health and disease". Oxidative Medicine and Cellular longevity, 2(5):270 – 278, (2009).

[10]. Dan Brennan MD "Healthy Foods High in Polyphenols", (2020).

[11]. A.N.Panche, A.D.Diwan and S.R.Chandra "Flavonoids: An overview". Nutritional Science, vol.5(1):1-5, (2016).

[12] Yang, C.S., Chung, J.Y., Yang, G.Y., Vhhabra, S.K., & Lee, M.J., Tea and tea polyphenols in cancer prevention. The journal of nutrition, Vol.130(2), (2000).

[13]. Dr.Nicola Tazzini "Flavonoids ; Chemical Structure, Classification and examples" Biotechnology, (2014).

[14]. Kwaku G. Duodu and Joseph M. Awika "Phytochemical-Related Health-Promoting Attributes". Sorghum and Millets-Second Edition, (2019).

[15]. M. Herrero and E. Ibanez "Extraction Techniques and Applications: Food and Beverage". Molecular Science, vol.4(1):225-258, (2012).

[16]. Irene Dini "An Overview of Functional Beverages". Biotechnology, vol.11(1):(1 – 40), (2019).

[17]. Belen Pastor-Villaescusa, Estefania Sanchez Rodriguez and Oscar D.Rangel-Huerta "Polyphenols in Obesity and Metabolic Syndrome". Molecular Physics,vol.11(1):213 – 239, (2018).

[18]. YusufYilmaz "Novel uses of catechins in foods". Biotechnology,vol.17(1):64 – 71, (2006).

[19]. Joonseo Bae, Nayoung Kim, Yunyoung Shin, Soo-Yeon Kim and You-Jeong Kim "Activity of catechins and their applications". Biomedical dermatology, vol.4(8), (2020).

[20]. Sourav Das, Leader Langbang, Mahabul Haque, Vinay Kumar Belwal, Kripamoy Aguan, Atanu Singha Roy. "Biocompatible silver nanoparticles: An investigation into their protein binding efficacies, anti-bacterial effects and cell cytotoxicity studies". Journal of Pharmaceutical Analysis, vol.11:422-434 (2020)

[21]. IbrahimKhan, KhalidSaeed, IdreesKhan. "Nanoparticles: Properties, applications and toxicities". Arabian Journal of Chemistry, vol.12:908-931 (2019)

[22]. Sunil T. Galatage, Aditya S. Hebalkar, Shradhey V. Dhobale, Omkar R. Mali, Pranav S. Kumbhar, Supriya V. Nikade and Suresh G. Killedar. "Silver Nanoparticles: Properties, Synthesis, Characterization, Applications and Future Trends (2021)"

[23]. Zahid Hussain , Mohammed A.S. Abourehab, Shahzeb Khan and Hnin Ei Thu. "Silver nanoparticles: a promising nanoplatform for targeted delivery of therapeutics and optimized therapeutic efficacy". Metal Nanoparticles for Drug Delivery and Diagnostic Applications 141-173 (2020)

[24]. Xi-Feng Zhang, Zhi-Guo Liu, Wei Shen, and Sangiliyandi Gurunathan. "Silver Nanoparticles: Synthesis, Characterization, Properties, Applications, and Therapeutic Approaches". International Journal of Molecular Science, vol.17(9) (2016)

[25]. Athina Papadopoulou, Rebecca J Green, Richard A Frazier. "Interaction of flavonoids with bovine serum albumin: a fluorescence quenching study". Agric Food Chem, vol.53(1): 158-163 (2005)

[26]. AswathyRavindran, AmitavaMukherjee. "Studies on interaction of colloidal Ag nanoparticles with Bovine Serum Albumin (BSA)". Colloids and Surfaces B: Biointerfaces , vol.76:32-37 (2010)

[27]. MijunPeng, ShuyunShi, YupingZhang. Influence of Cd^{2+}, Hg^{2+} and Pb^{2+} on (+)-catechin binding to bovine serum albumin studied by fluorescence spectroscopic methods. Spectrochimica Acta Part A: Molecular and Biomolecular Spectroscopy, vol.85(1): 190-197 (2012)

[28]. Durba Roy, BITS Pilani, Hyderabad Samrajnee Dutta Shyam Sundar Maity Sanjib Ghos. "Spectroscopic and docking studies of the binding of two stereoisomeric antioxidant catechins to serum albumins". Article in Journal of Luminescence, vol.132: 1364-1375 (2012)

[29]. Skrt M, Benedik E, Podlipnik C, Ulrih NP. "Interactions of different polyphenols with bovine serum albumin using fluorescence quenching and molecular docking". Article in Food Chemistry vol.135(4): 2418-2424 (2012)

[30]. MihaelaSkrt, Natasa PoklarUlrih. "Interactions of different polyphenols with bovine serum albumin using fluorescence quenching and molecular docking". Food Chemistry, vol.135(4): 2418-2424 (2012)

[31]. SaurabhGautam, PriyankaDubey, Munishwar N.Gupta. "A facile and green ultrasonic-assisted synthesis of BSA conjugated silver nanoparticles".Colloids and Surface B: Biointerfaces, vol.102:879-888 (2013)

[32]. XiangrongLi, YongbingHao. "Probing the binding of (+)-catechin to bovine serum albumin by isothermal titration calorimetry and spectroscopic techniques". Journal of Molecular Structure vol.1091 :109-117 (2015)

[33]. P.Chowdhury, T.Bora, S.A.Khan, B.Chakraborty, K.Senapati, M.Sengupta, S.Borchetia, T.Bandyopadhyay."Inhibition of Japanese encephalitis virus infection by biogenic catechin silver nanoparticles: An in-vitro study". International Journal of Infectious Diseases, vol.45:275-276 (2016)

[34]. AdityBose. “Interaction of tea polyphenols with serum albumins: A fluorescence spectroscopic analysis”. Journal of Luminescence, vol.169:220-226 (2016)

[35]. MunevverSokmen, Suliman YousufAlomar, CansuAlbay, GonulSerdar. “Microwave assisted production of silver nanoparticles using green tea extracts”. Journal of Alloys and Compounds vol.725:190-198 (2017)

[36]. Nada ShaeelAL-Thabaiti, Maqsood AhmadMalik, ZaheerKhan. “Protein interactions with silver nanoparticles: Green synthesis, and biophysical approach”. International Journal of Biological Macromolecules, vol.95:421-428 (2017)

[37]. T. Fafal, P. Taştan, B.S. Tüzün, M. Ozyazici, Bijen Kivcak. “Synthesis, characterization and studies on antioxidant activity of silver nanoparticles using Asphodelus aestivus Brot. aerial part extract”. South African Journal of Botany, vol.112:346-353 (2017)

[38]. Siddhant Jain & Mohan Singh Mehata. “Medicinal Plant Leaf Extract and Pure Flavonoid Mediated Green Synthesis of Silver Nanoparticles and their Enhanced Antibacterial Property”. Scientific Report, vol.7(1) (2017)

[39]. KatarzynaRanoszek-Soliwoda, JaroslawGrobelny. “The synthesis of monodisperse silver nanoparticles with plant extracts”. Colloids and Surfaces B: Biointerfaces, vol.177:19-24 (2019)

[40]. P.ChanphaiH., A.Tajmir-Riahi. “Tea polyphenols bind serum albumins:A potential application for polyphenol delivery”. Food Hydrocolloids, vol.89:461-467 (2019)

[41]. Sourav Das, Leader Langbang, Mahabul Haque, Vinay Kumar Belwal, Kripamoy Aguan, Atanu Singha Roy. “Biocompatible silver nanoparticles: An investigation into their protein binding efficacies, anti-bacterial effects and cell cytotoxicity studies”. Journal of Pharmaceutical Analysis, vol.11:422-434 (2020)

[42]. Anitha.S, Saranya.V., Shankar.R, Sasirekha.V. “Structural exploration of interactions of (+) catechin and (−) epicatechin with bovine serum albumin: Insights from molecular dynamics and spectroscopic methods”. Journal of Molecular Liquids, vol.348:118026 (2021)

[43]. SedighehHashemnia, HajarZarei, ZaynabMokhtari, Mohammad HosseinMokhtari. “An investigation of the effect of PVP-coated silver nanoparticles on the interaction between clonazepam and bovine serum albumin based on molecular dynamics simulations and molecular docking”. Journal of Molecular Liquids, vol.323:114915 (2021)

[44]. A.Kavitha, S.Ravichandran. "Synthesis and enhanced antibacterial using plant extracts with silver nanoparticles: Therapeutic application". Inorganic Chemistry Communications, vol.134:109045 (2021)

[45]. Tiantian Zhang , Tao Wei , Yuanyuan Han, Heng Ma, Mohammadreza Samieegohar, Ping-Wei Chen, Ian Lian and Yu-Hwa Lo. Protein–Ligand Interaction Detection with a Novel Method of Transient Induced Molecular Electronic Spectroscopy (TIMES): Experimental and Theoretical Studies, vol.2:834-842 (2016)

[46]. S. Sreedhanya, V.R. Jeena, S. Ammu, C.T. Aravindakumar , Usha K. Aravind. "Spectroscopic and theoretical methods to probe protein–ligand binding". Materials Today: Proceedings, vol.33:1361-1366 (2020)

[47]. Farhat Ikram, Amtul Qayoom, Muhammad Raza Shah. "Synthesis of Epicatechin Coated Silver Nanoparticles for Selective YRecognition of Gentamicin". Sensors and Actuators B, vol.257:897-905 (2017)

[48]. Justin Tom.UV-Vis-spectroscopy-principle-strengths-and-limitations-and-applications"

Analysis & Separations (2021)

[49]. Md Abrar Siddiquee, Mehraj ud din Parray, Syed Hassan Mehdi, KhalidAhmed Alzahrani, Abdulmohsen Ali Alshehri, Maqsood Ahmad Malik, Rajan Patel. "Green synthesis of silver nanoparticles from Delonix regia leaf extracts: In-vitro cytotoxicity and interaction studies with bovine serum albumin". Material Chemistry and Physics, vol.242:122493 (2020)

[50]. Siddhant Jain & Mohan Singh Mehata. "Medicinal Plant Leaf Extract and Pure Flavonoid Mediated Green Synthesis of Silver Nanoparticles and their Enhanced Antibacterial Property". Scientific Report (2017)

[51]. T. Fafal, P. Taştan , B.S. Tüzün, M. Ozyazici , Bijen Kivcak. "Synthesis, characterization and studies on antioxidant activity of silver nanoparticles using Asphodelus aestivus Brot. aerial part extract". South African Journal of Botany, vol.112:346-353 (2017)

[52]. X. Li, Y. Hao, "Probing the binding of (+) -catechin to bovine serum albumin by isothermal titration calorimetry and spectroscopic techniques", J. Mol. Struct, vol.1091:109-117 (2015)

[53]. S.Das, N.Bora, M. A.Rohman, R.Sharma, A.N. Jha, A.S. Roy, "Molecular recognition of bio-active flavonoids quercetin and rutin by bovine hemoglobin: An overview of the binding mechanism, thermodynamics and structural aspects through multi-spectroscopic and molecular dynamics simulation studies"**,** Phys. Chem. Chem. Phys**, v**ol**.**20:21668-21684 **(**2018)

[54]. Prakash Periakaruppan, P.Gnanaprakasam, Roham Emmanual, Arokiyaraj Selvaraj "Green synthesis of silver nanoparticles from leaf extract of Mimusops". Colloids & Surface B: Biointerfaces, vol.108:255-259 (2012)

[55]. A. Bhogale, N. Patel, J. Mariam, P. Dongre, A. Miotello, D. Kothari, "Comprehensive studies on the interaction of copper nanoparticles with bovine serum albumin using various spectroscopies", Colloids and Surfaces B: Biointerfaces, vol.113:276-284 (2014)

[56]. R. Binaymotlagh, H. Hadadzadeh, H. Farrokhpour, F.H. Haghighi, F. Abyar, S.Z. Mirahmadi-Zare, "In situ generation of the gold nanoparticles–bovine serum albumin (AuNPs–BSA) bioconjugated system using pulsed-laser ablation (PLA)", Materials Chemistry and Physics, vol.177: 360-370 (2016)

[57]. D. Roy, S. Dutta, S. Sundar Maity, S. Ghosh, A. Singha Roy, K. Sundar Ghosh, S. Dasgupta, "Spectroscopic and docking studies of the binding of two stereoisomeric antioxidant catechins to serum albumins", Journal of Luminescence, vol.132:1364-1375 (2012)

[58]. R. Binaymotlagh, H. Hadadzadeh, H. Farrokhpour, F.H. Haghighi, F. Abyar, S.Z. Mirahmadi-Zare. "In situ generation of the gold nanoparticles–bovine serum albumin (AuNPs–BSA) bioconjugated system using pulsed-laser ablation (PLA)", Materials Chemistry and Physics, vol.177:360-370 (2016)